2016-06-01

Typical and Darkened Portland Cement Concrete Pavement: Temperature, Moisture, and Roughness Analyses

Tenli Waters
Brigham Young University

Typical and Darkened Portland Cement Concrete Pavement:

Temperature, Moisture, and Roughness Analyses

Tenli Waters

A thesis submitted to the faculty of
Brigham Young University
in partial fulfillment of the requirements for the degree of

Master of Science

W. Spencer Guthrie, Chair
Mitsuru Saito
Brian Mazzeo

Department of Civil and Environmental Engineering

Brigham Young University

June 2016

ABSTRACT

Typical and Darkened Portland Cement Concrete Pavement:
Temperature, Moisture, and Roughness Analyses

Tenli Waters
Department of Civil and Environmental Engineering, BYU
Master of Science

The objectives of this research were to 1) investigate the effects of lower concrete albedo on the thermal behavior of concrete pavement by directly comparing temperatures and moisture contents of typical and darkened concrete pavements and 2) investigate changes in roughness of both typical and darkened concrete pavements as a result of changes in temperature and moisture gradients. The scope of the research included instrumentation, testing, and analysis of typical and darkened concrete pavements constructed in northern Utah.

Procedures related to field testing included infrared thermography, thermocouple readings, sensor data collection, and roughness surveys. Elevation surveys and albedo measurements were also performed to further characterize the site. Procedures related to laboratory testing included elastic modulus, compressive strength, rapid chloride permeability, thermal conductivity, and Schmidt rebound hammer testing of cylinders prepared from typical and darkened concrete.

When considered over the entire monitoring period, the average surface temperatures of the darkened pavement were higher than those of the typical pavement by 3.3°F, and the average subsurface temperatures of the darkened pavement were higher than those of the typical pavement by 3.1°F. A strong positive correlation exists between the air temperature and both the surface and the subsurface pavement temperatures. The difference between both the surface and subsurface temperatures of the darkened and typical pavements decreases as the air temperature decreases. The results of a simple linear regression suggest that, when the air temperature is 32°F, the surface temperature of the darkened concrete is just 0.2°F higher than that of the typical concrete and the subsurface temperature of the darkened concrete is 1.1°F higher than that of the typical concrete. The difference in surface temperature is expected to be 0°F when the air temperature is 30.5°F, while the difference in subsurface temperature is expected to be 0°F when the air temperature is 17.9°F. Therefore, the darkened pavement is unlikely to melt snow and ice faster than the typical pavement or provide significantly greater frost protection to subsurface layers and buried utilities during winter for conditions similar to those in this research.

The roughness measurements for the typical pavement exhibit much more daily variability than seasonal variability. The roughness measurements for the darkened pavement also exhibit more daily variability than seasonal variability but less overall variability than that of the typical pavement. Neither pavement temperature gradient nor moisture gradient appears to be correlated to roughness for either the typical pavement or the darkened pavement.

Key words: concrete pavement, curling, moisture gradient, roughness, temperature gradient, warping

ACKNOWLEDGEMENTS

TABLE OF CONTENTS

LIST OF TABLES

LIST OF FIGURES

1   INTRODUCTION

1.1   Problem Statement

While portland cement concrete pavement offers a durable surface and long service life when designed and constructed properly, concrete pavement sections can require more expensive winter maintenance treatments to clear snow and ice in cold regions than asphalt pavement sections (Guthrie et al. 2014). One method of potentially reducing winter maintenance costs is darkening the concrete pavement; however, little research exists on the use of this method. Darkening the concrete reduces its albedo, or whiteness, and would therefore be expected to change its thermal behavior. Although research describing the thermal behavior of asphalt and typical concrete pavements has been published (Guthrie et al. 2014, Yavuzturk et al. 2005), studies on the thermal behavior of darkened concrete pavement have not been identified in the literature review performed for this research.

Darkened concrete should promote higher pavement surface temperatures through increased absorption of radiation energy from the sun (Gajda and Van Geem 1997). Radiation is one of three primary heat transfer mechanisms, which also include conduction and convection (Wang 2015). Radiation refers to short-wave solar radiation transferred from the sun to the pavement surface. Conduction refers to the transfer of heat between pavement layers and is dependent on the thermal conductivity of the pavement system. Convection refers to the transfer of heat between the surface of the pavement system and the surrounding environment; in

particular, wind speed can have an effect on this method of heat transfer (Wang 2015). While greater solar radiation leads to higher pavement surface temperatures, greater convection generally leads to lower temperatures. However, the effect of conduction depends on the surrounding conditions, where heat transfer occurs from areas of higher temperature to areas of lower temperature.

To the extent that the combination of these heat transfer mechanisms generates higher surface temperatures of darkened concrete pavement during the winter season, darkened concrete pavement should melt snow and ice more quickly, all other factors the same, than typical concrete pavement. In addition to increasing the surface temperature, darkened concrete should also increase the subsurface temperature of the pavement and therefore potentially provide greater frost protection to subsurface layers and buried utilities during winter in cold regions. However, higher surface temperatures may generate higher thermal gradients through the depth of the slab, causing greater slab curling (Nassiri and Vandenbossche 2011). Higher surface temperatures may also lead to higher moisture gradients through the depth of the slab, causing greater slab warping.

Both curling and warping of concrete slabs can lead to a rougher pavement surface (Siddique et al. 2003, Siddique et al. 2004); roughness is an important factor in pavement serviceability assessment, as it has a large impact on the traveling public. Slab curling and warping also create greater internal concrete stresses and, when traffic loads are applied, can lead to cracking of the concrete (Belshe et al. 2011, Choubane and Tia 1995, Huang 2004, Lange et al. 2006). Limited research has been performed to address the effects of curling and warping on roughness of darkened concrete pavement.

1.2   Research Objectives and Scope

The objectives of this research were to 1) investigate the effects of lower concrete albedo on the thermal behavior of concrete pavement by directly comparing temperatures and moisture contents of typical and darkened concrete pavements and 2) investigate changes in roughness of both typical and darkened concrete pavements as a result of changes in temperature and moisture gradients. The scope of the research included instrumentation, testing, and analysis of typical and darkened concrete pavements constructed in northern Utah.

1.3   Report Outline

Five chapters are included in this report. Chapter 1 gives the problem statement and outlines the objectives of this research, and Chapter 2 provides relevant background information. Chapters 3 and 4 present the research procedures and results, respectively, and Chapter 5 gives conclusions and recommendations based on the research findings. Additional data are included in Appendices A and B.

2 BACKGROUND

2.1 Overview

Developed from a literature review performed for this research, the following sections describe safety and winter maintenance, pavement albedo, tinted concrete, pavement temperature and moisture, curling and warping, and pavement roughness.

2.2 Safety and Winter Maintenance

When bonded to pavements, snow and ice are extremely hazardous to drivers; therefore, removal of snow and ice is the focus of most winter maintenance programs in cold regions. For example, northern Utah experiences severe winters, requiring the Utah Department of Transportation (UDOT) to remove about 65,000,000 tons of snow from state highways in a typical winter (UDOT 2011). UDOT uses winter maintenance strategies such as plowing and salt application to manage winter road conditions (Guthrie and Thomas 2014, Sumsion and Guthrie 2013).

In a previous study performed for UDOT, asphalt and concrete pavement surface temperatures were compared at a location on U.S. Route 40 in northern Utah where asphalt and concrete met end to end at the base of a mountain pass. The results of this study indicated that, at low air temperatures, the concrete pavement had lower surface temperatures than the asphalt pavement and would therefore be expected to experience freezing before the asphalt pavement

(Guthrie et al. 2014). Consequently, for pavement material properties and environmental conditions similar to those evaluated in that study, concrete pavement would require more winter maintenance, on average, than asphalt pavement. Higher asphalt pavement temperatures due to a lower albedo are anticipated to reduce the amount of snow and ice accumulation and therefore potentially allow for a reduction in winter maintenance costs.

2.3   Pavement Albedo

Albedo is the ratio of reflected solar radiation to the incoming solar radiation from the sun and is measured on a scale of 0.0 to 1.0. Materials having a lower albedo absorb more solar radiation, while materials having a higher albedo absorb less solar radiation (Gajda and Van Geem 1997, Li et al. 2013). Typical concrete albedo values range from approximately 0.26 to 0.35 (Boriboonsomsin and Reza 2008, Guthrie et al. 2016, Wang 2015), while typical asphalt albedo values range from approximately 0.05 to 0.17 (Richard et al. 2015). Variation in pavement albedo can occur throughout the day, as well as throughout the year, as a result of changes in pavement surface conditions, such as the presence of moisture and/or debris, and changes in solar radiation intensity (Li et al. 2013).

Much of the literature focusing on the albedo of pavements addresses high temperature with respect to the urban heat island (UHI) effect, which is a localized increase in air temperature due to high pavement surface temperature resulting from a high density of low-albedo pavements, such as asphalt, in a city (Pomerantz et al. 1997). A higher albedo is desirable to reduce the UHI effect (Asaeda et al. 1995, Levinson and Akbari 2002, Li et al. 2013, Pomerantz et al. 1997, Pomerantz et al. 2000a, Pomerantz et al. 2000b, Pomerantz et al. 2003, Richard et al. 2015, Synnefa et al. 2009, Ting et al. 2001, Wong et al. 2009). However, little information exists in

the literature on the use of lower-albedo materials to increase pavement surface temperature for the purpose of melting snow and ice.

2.4 Tinted Concrete

The use of tinted concrete for achieving specific aesthetic qualities, generally for architectural purposes, is common (Paris and Chusid 1999). Typical pigments for tinting concrete include red mud from the aluminum industry, titanium dioxide, zinc oxide, zinc phosphate, micronized talc, diatomaceous silica, micronized calcium carbonate, and barite (Pera et al. 1997, Youssef et al. 1998). Iron oxide, the pigment used in this research, is also available for tinting concrete, and its darkening effect on the thermal behavior of concrete pavement, especially with respect to freezing conditions, is the focus of this research.

2.5 Pavement Temperature and Moisture

Different pavement surfaces have different albedos and may therefore experience different temperatures under similar environmental conditions. During the winter season, when pavements are exposed to freezing air temperatures, the pavement surface temperature can influence the amount of ice that forms (Guthrie et al. 2014).

Vertical temperature and moisture gradients occur within the concrete pavement layer because the top of the concrete is exposed to different conditions than the bottom of the concrete (Lange et al. 2006, Nassiri and Vandenbossche 2011). Variability in temperature and moisture between the top and bottom surfaces of the concrete layer often occur due to exposure of the top surface to changing air temperature, solar radiation, and relative humidity, while the bottom surface is relatively insulated from these effects by the overlying concrete. Therefore, the

6

temperature and moisture content at the top surface of the concrete pavement typically fluctuate much more widely than the temperature and moisture content at the bottom surface of the concrete (Nassiri and Vandenbossche 2011), which causes dynamically changing temperature and moisture gradients within the concrete layer.

2.6   Curling and Warping

Curling and warping of concrete slabs result from vertical temperature and moisture gradients, respectively (Armaghani et al. 1987, Nassiri and Vandenbossche 2011). Slabs tend to curl and/or warp toward the cooler and/or drier surface, causing the corners of the slab to lift or drop relative to the center of the slab depending on the gradients (Nassiri and Vandenbossche 2011). Consequently, curling and warping can cause tensile stresses in the concrete that lead to accelerated cracking under trafficking (Lange et al. 2006, Nassiri and Vandenbossche 2011).

2.7   Pavement Roughness

Pavement roughness, which is an indicator of both rider comfort and safety, refers to the ride quality of a pavement surface and is mainly controlled by the longitudinal profile of the road (Siddique et al. 2003). Pavements naturally have some roughness built in as a result of construction; some pavements have higher built-in roughness than others (Siddique et al. 2004). Because curling and warping affect the flatness of concrete slabs, increased roughness may also result from curling and warping of concrete pavement (Siddique et al. 2003, Siddique and Hossain 2005). In one study, as much as 39 percent of the total pavement roughness was attributed to curling (Siddique et al. 2003). Curling and warping can be reduced by using proper joint spacing, increasing the slab thickness, adding reinforcement, increasing concrete compressive strength, and reducing the overall concrete shrinkage, including using a concrete

aggregate that is less susceptible to thermal expansion and contraction (Mailvaganam et al. 2000, Siddique and Hossain 2005).

2.8   Summary

A literature review was performed in this research to investigate safety and winter maintenance, pavement albedo, tinted concrete, pavement temperature and moisture, curling and warping, and pavement roughness. When bonded to pavements, snow and ice are extremely hazardous to drivers; therefore, removal of snow and ice is the focus of most winter maintenance programs in cold regions. Higher asphalt pavement temperatures due to a lower albedo are anticipated to reduce the amount of snow and ice accumulation and therefore potentially allow for a reduction in winter maintenance costs. Iron oxide, the pigment used in this research, lowers the albedo of concrete, and its effect on the thermal behavior of concrete pavement, especially with respect to freezing conditions, was the focus of this research. Little information exists in the literature on the use of lower-albedo materials to increase pavement surface temperature for the purpose of melting snow and ice. Vertical temperature and moisture gradients occur within the concrete pavement layer because the top of the concrete is exposed to different conditions than the bottom of the concrete. Curling and warping of concrete slabs result from vertical temperature and moisture gradients, respectively. Because curling and warping affect the flatness of concrete slabs, increased roughness may also result from curling and warping of concrete pavement.

3   PROCEDURES

3.1   Overview

The following sections describe the site layout and instrumentation and the procedures followed for field and laboratory testing.

3.2   Site Layout

UDOT directed construction of a new 9-in.-thick concrete pavement, reinforced with steel dowels and tie bars, along 1000 West in Logan, Utah, during the summer of 2013. At the intersection of 1000 West and 1400 North, one section each of typical and darkened concrete pavement was placed on the west side, while two sections each of typical and darkened concrete pavement were placed on the east side. These sections were labeled as sites 1 through 3 as illustrated in Figure 3-1. In Figures 3-1, 3-2, and 3-3, the absence of hatching and shading indicates a typical concrete section, hatching indicates a darkened concrete section, and solid gray indicates asphalt pavement.

3.3   Site Instrumentation

Both the typical and the darkened concrete pavement sections were instrumented with temperature and moisture sensors, as shown in Figures 3-2 and 3-3, to enable monitoring of surface and subsurface temperatures and moisture contents at hourly intervals. At one typical and one darkened concrete pavement section on each side of the intersection, one location within
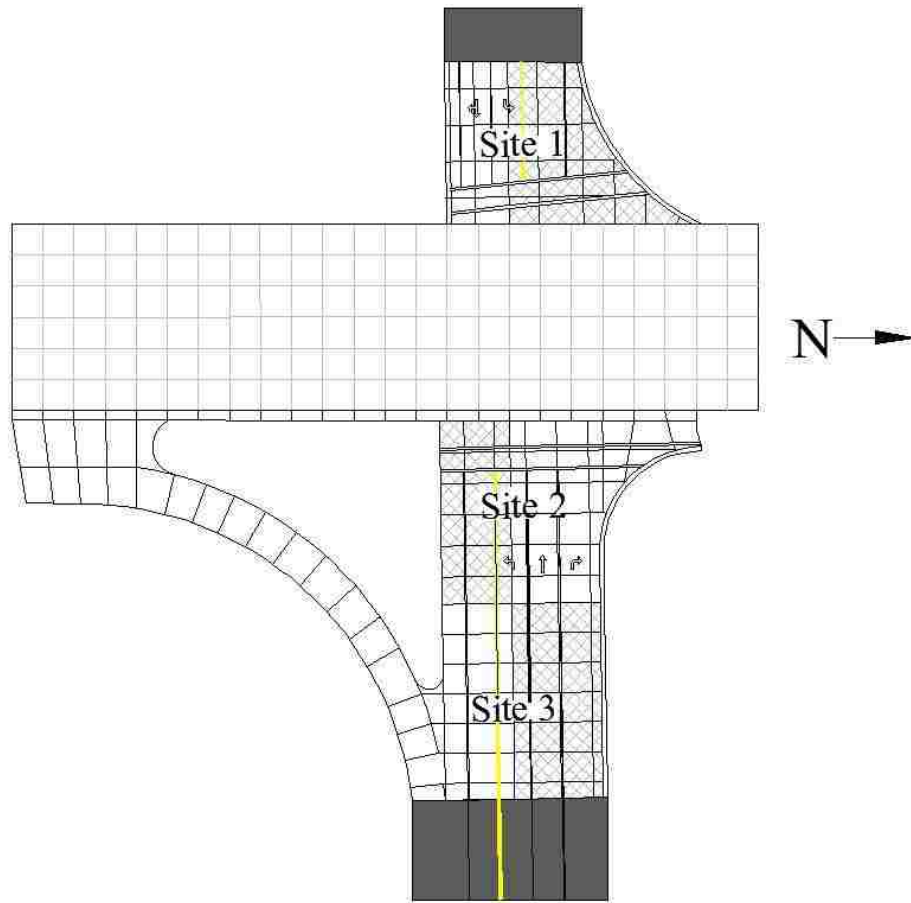
Figure 3-1: Intersection layout of 1000 West 1400 North.

a wheel path was selected for installation of sensors at the top and bottom of the concrete slab; measuring temperature and moisture at both the top and bottom of the concrete slabs allowed for computation of the temperature and moisture gradients at the selected locations. To position the sensors at the desired depths, the researchers mounted them on a non-conductive plastic stake secured in the subbase prior to concrete placement as shown in Figure 3-4; the sensors were 1.25 in. in height and were placed 7.25 in. apart so that approximately 0.25 in. of clear space would exist between the sensors and the top and bottom of the concrete slab. The sensor cables were carefully routed through 0.75-in.-diameter polyvinyl chloride (PVC) pipe that was buried just below the surface of the subbase layer as shown in Figure 3-5. On each side of the intersection,

10

● Thermocouple between Concrete and Subbase

□ Upper and Lower Temperature and
Moisture Sensors in Concrete
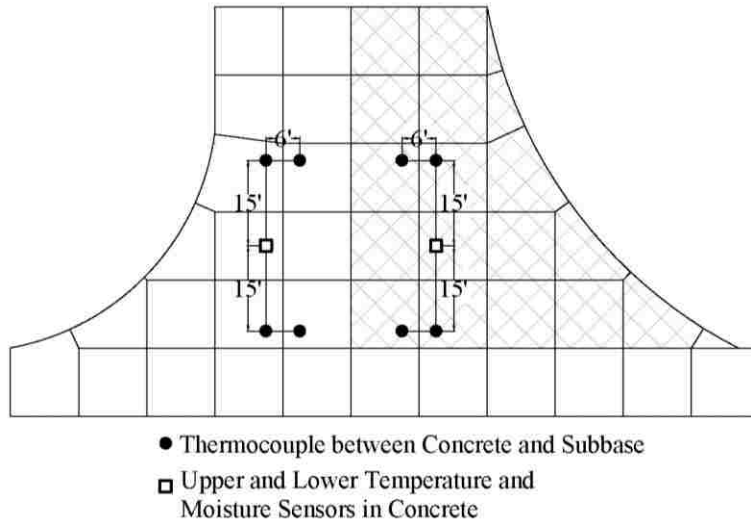
Figure 3-2: Site 1 sensor and thermocouple layout.

● Thermocouple between Concrete and Subbase

□ Upper and Lower Temperature and
Moisture Sensors in Concrete
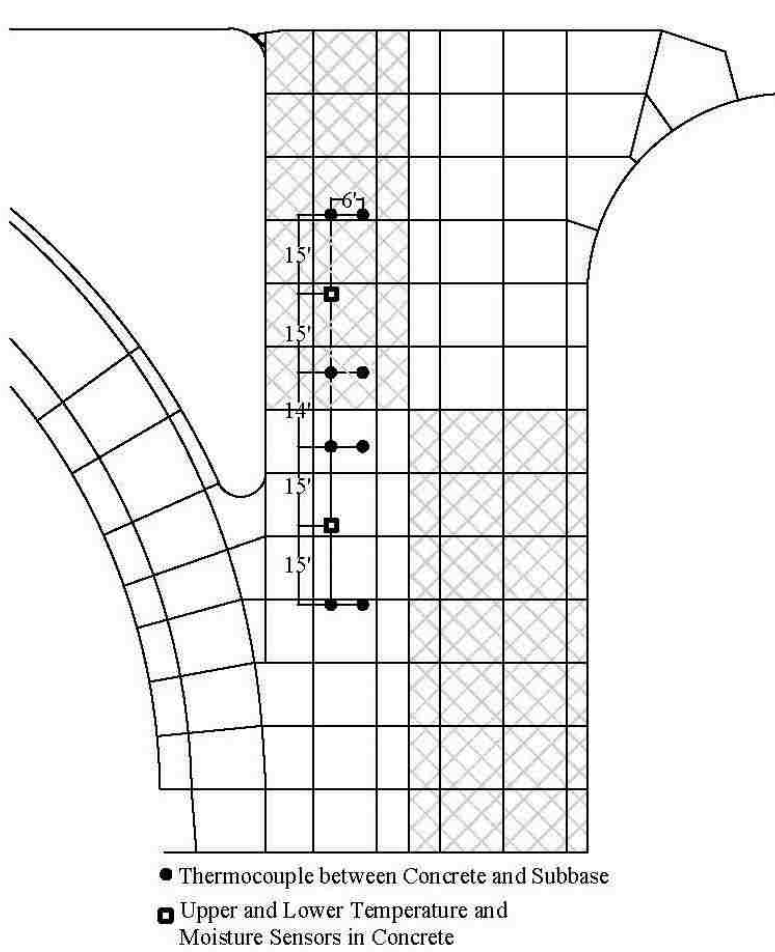
Figure 3-3: Sites 2 and 3 sensor and thermocouple layout.

11

Figure 3-4: Temperature and moisture sensors for monitoring concrete pavement.

Figure 3-5: Sensor cables in PVC pipe.

the PVC pipe conveyed the cables from the sensor locations to a nearby signal pole, where thecables were terminated in a steel utility box mounted approximately 12 ft high as shown in Figure 3-6.

In addition to the sensors in the concrete, environmental sensors were installed to measure ambient conditions, including air temperature, relative humidity, and precipitation. These sensors were mounted to the signal poles 1 to 2 ft above the utility boxes, and the cables were routed to the utility boxes through conduit for protection. Inside the utility box, each cable was connected to a battery-powered data logger that was programmed to collect data from the sensors on an hourly basis and send the data to a remotely accessible database through a daily

Figure 3-6: Utility box mounted on signal pole.

cellular transmission. In this way, data could be continuously collected even in the absence of the researchers.

To supplement the temperature and moisture sensors near the bottom of the concrete, four thermocouple wires were also placed at the interface of the subbase and the concrete within each of the same sections; the layouts of these thermocouples are shown in Figures 3-2 and 3-3. In each section, two thermocouples were placed in the same wheel path as the sensors mounted to the stake, while the other two thermocouples were placed in the other wheel path. The thermocouple wires were housed in PVC pipe or protective foam sleeves and routed to the same utility boxes where they could be easily accessed for manual reading during site visits by the researchers.

3.4 Pavement Construction

After the temperature and moisture sensors and the thermocouple wires were all installed, either typical or darkened concrete was placed in each section by the contractor selected by UDOT for this project. For both concrete mixtures, the design water-cementitious material ratio was 0.42, a 20 percent replacement of portland cement with fly ash was specified, and the entrained air content was 6 percent. The only difference between the two mixtures was that, for the darkened concrete, iron oxide pigment was added in the amount of 4 percent by weight of total cementitious material, corresponding to the addition of approximately 25 lb of iron oxide per cubic yard of concrete; this was the maximum amount suggested by the manufacturer to make the darkened concrete as dark as possible and resulted in an increase of approximately $60 per cubic yard of concrete. Use of an integral tint rather than a surficial application ensured that

wear from trafficking and possible future grinding to change lane striping, for example, would

not compromise the darkened surface.

Concrete was placed on the west and east sides of the intersection during July and

September 2013, respectively. Figure 3-7 shows placement of the darkened concrete in site 2. A

concrete sample was collected in a wheelbarrow from the pump hose immediately after concrete

was placed around the temperature and moisture sensors previously placed in each of the

instrumented sections; this practice ensured that the sampled concrete was representative of the

concrete surrounding the sensors. The researchers cast 10 4-in. by 8-in. cylinders of each type of

concrete on each side of the intersection during placement. In addition, the researchers cast two

6-in. by 12-in. cylinders of each type of concrete on the east side. The cylinders were allowed to

Figure 3-7: Placement of darkened concrete.

cure for at least 24 hours on site before being carefully transported to the Brigham Young University (BYU) Highway Materials Laboratory for testing. After approximately 24 hours of curing, the concrete joints were saw-cut on approximately 12-ft intervals in both the transverse and longitudinal directions.

3.5   Field Testing

Following construction of the pavement sections, the researchers returned to the site for additional testing on regular intervals of 3 to 4 months. Specifically, they performed testing in November 2013, February 2014, June 2014, and September 2014. During each site visit, they performed testing at four or five different times during a given 24-hour period. This testing schedule was designed to enable evaluation of complete daily solar cycles within different seasons so that the two types of concrete pavement could be compared in a variety of environmental conditions. Procedures related to field testing included infrared thermography, thermocouple readings, sensor data collection, and roughness surveys. Elevation surveys and albedo measurements were also performed to further characterize the site.

3.5.1   Elevation Surveys

Transverse and longitudinal slopes were measured during June 2015 using surveying equipment, as shown in Figure 3-8. Elevations were measured around the perimeter of the main lanes in each section at 5-ft intervals in the transverse direction and at 10-ft intervals in the longitudinal direction.

Figure 3-8: Measurement of roadway elevations.

3.5.2 Albedo Measurements

Albedo values were measured in general accordance with American Society for Testing and Materials (ASTM) E1918 (Standard Test Method for Measuring Solar Reflectance of Horizontal and Low-Sloped Surfaces in the Field) during August 2015, at which point the surface of the pavement was considered to be representative of its long-term condition. Measurements were taken using a pyranometer, shown in Figure 3-9, set up normal to the surface of the pavement with the center of the probe approximately 60 in. above the surface of the pavement. Monitoring of the albedo over time was not possible in this research due to limited equipment availability.

A total of six readings were taken in each of the typical and darkened concrete sections within site 1. Within each section, three test locations were established, and testing in both the dry and wet conditions was performed at each test location. For the typical section, testing was performed at 10-ft intervals along a line extending east from a point approximately 3 ft north of

17

Figure 3-9: Measurement of pavement albedo.

the southwest corner of the section. For the darkened section, testing was performed at 10-ft

intervals along a line extending east from a point approximately 3 ft south of the northwest

corner of the section. After the first reading was taken with the pavement in a dry condition, the

measurement area was sprayed with water, and a second reading was taken in a wet condition;

the surface was re-sprayed as needed to ensure that the pavement surface remained wet during

testing.

For comparison, albedo measurements of the asphalt adjacent to site 1 were also taken in

dry and wet conditions. For the asphalt, testing was performed at approximately 22-ft intervals

along a line extending south from a point approximately 10 ft west of the northwest corner of the

darkened section.

3.5.3   Infrared Thermography

At each testing time, the researchers documented surface temperatures using infrared thermography, as shown in Figure 3-10. The infrared photographs were mainly focused on the instrumented regions of the pavement so that the surface temperatures measured using the infrared thermography would be spatially correlated to the subsurface temperatures measured using thermocouples. The infrared images were analyzed using commercial software to determine average pavement surface temperatures in the regions of interest.

Figure 3-10: Measurement of surface temperatures using infrared thermography.

3.5.4   Thermocouple Readings

At each testing time, the researchers recorded the subsurface temperatures as measured using the thermocouple wires. Thermocouple readings were obtained manually using a thermocouple reader as shown in Figure 3-11.

Figure 3-11: Measurement of subsurface temperatures using thermocouple reader.

3.5.5   Sensor Data Collection

To obtain the sensor data, including pavement temperature and moisture and air temperature, relative humidity, and precipitation, the researchers remotely downloaded data from the data loggers approximately bi-weekly for a period of two years. In addition, the researchers obtained solar radiation and wind speed data measured hourly at the Campbell Scientific, Inc. headquarters, which was approximately half a mile from the research site. All of the data were compiled in a spreadsheet for analysis.

3.5.6   Roughness Surveys

At each testing time, pavement roughness surveys were performed in general accordance with ASTM E1364 (Standard Test Method for Measuring Road Roughness by Static Level Method) using a roadway profiler in the wheel paths of each section, as shown in Figure 3-12. To ensure that the survey began in exactly the same location and proceeded along the same line in each case, the researchers permanently marked the beginning and ending points of each line and the exact placement of the profiler at the beginning point, as shown in Figure 3-13. This process ensured that variability between successive measurements in the same wheel path could be attributed to either temperature curling and/or moisture warping of the tested slab.
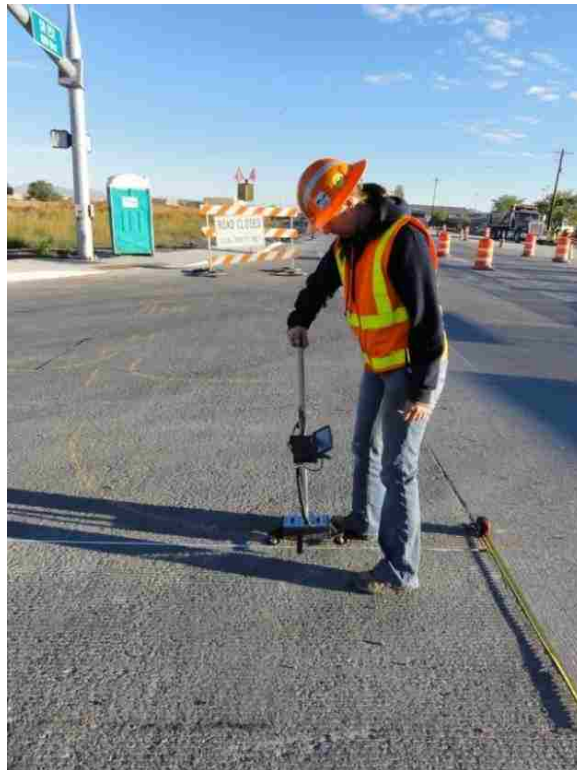
Figure 3-12: Measurement of pavement roughness using a roadway profiler.

Figure 3-13: Marked beginning point on pavement for roughness survey.

3.6 Laboratory Testing

Procedures related to laboratory testing included elastic modulus, compressive strength, rapid chloride permeability, thermal conductivity, and Schmidt rebound hammer testing of cylinders prepared from typical and darkened concrete. After the initial 24-hour curing period on site, all cylinders were transported to the BYU Highway Materials Laboratory, immediately removed from their molds, and stored in a fog room with 100 percent humidity at approximately 85°F until they were tested.

3.6.1 Elastic Modulus Testing

As an assessment of the elastic modulus of the typical and darkened concrete, non-destructive free-free resonant tests were conducted on two cylinders of each concrete type measuring 4 in. in diameter and 8 in. in height at 7 days, 28 days, 6 months, and 1 year. The free-free resonant testing was performed immediately before compressive strength testing.

For free-free resonant testing, each concrete cylinder was placed on a stand as depicted in Figure 3-14, and the upper end of the cylinder was tapped lightly with a small hammer instrumented with a load cell that triggered data acquisition by an attached computer. An accelerometer mounted in a foam disk placed beneath the cylinder measured the amplitude and frequency of the stress waves induced in the concrete by the hammer strike, and the data were recorded and analyzed by the computer. Eight frequency measurements, as well as the length, diameter, and weight, were recorded for each cylinder. These values were used in the calculation of elastic modulus according to Equation 3-1 (Richart et al. 1970):

$$E = \frac{\frac{\gamma}{32.2} \cdot (2 \cdot l \cdot f)^2}{144}$$ (3-1)

where:

E = elastic modulus (psi)
γ = density (lb/ft^3)
l = length (ft)
f = frequency (Hz)

3.6.2 Compressive Strength Testing

Compressive strength tests were performed at 7 days, 28 days, 6 months, and 1 year on the same cylinders used in elastic modulus testing. The cylinders were capped with sulfur according to ASTM C617 (Standard Practice for Capping Cylindrical Concrete Specimens), and testing was then performed in general accordance with ASTM C39 (Standard Test Method for Compressive Strength of Cylindrical Concrete Specimens). The cylinders were tested at a strain rate of 0.05 in./minute as illustrated in Figure 3-15.
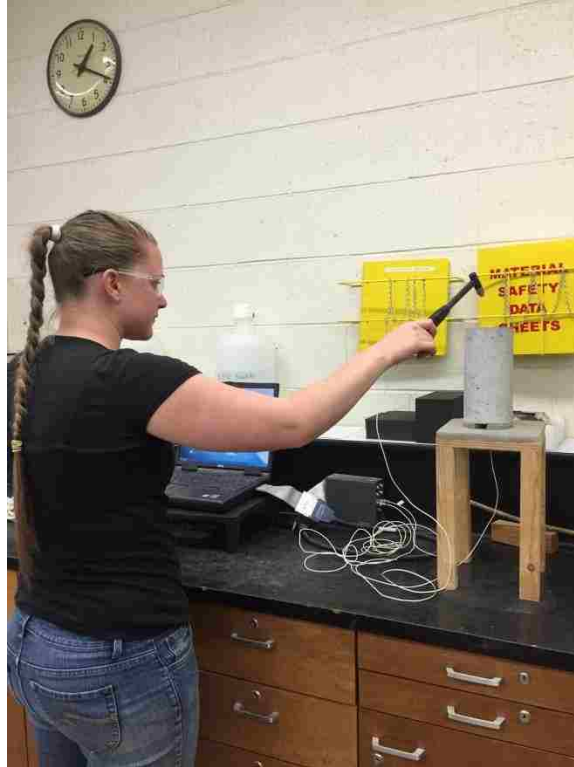
Figure 3-14: Elastic modulus testing.

Figure 3-15: Compressive strength testing.

3.6.3 Rapid Chloride Permeability Testing

Rapid chloride permeability testing was performed on two cylinders of each concrete type measuring 4 in. in diameter and 8 in. in height at 28 days, 6 months, and 1 year. Testing was done in general accordance with ASTM C1202 (Standard Test Method for Electrical Indication of Concrete's Ability to Resist Chloride Ion Penetration). Test samples were cut to a thickness of 2 in. from the middle of the cylinders using a masonry saw, so that three samples per cylinder were obtained. The samples were then saturated for a period of 24 hours in de-aired, de-ionized water. After the conditioning period was complete, the opposite faces of eachspecimen were exposed to solutions of sodium hydroxide and sodium chloride while a 60V potential was imposed over the length of the specimen. During the 6-hour test, the total charge, in coulombs, that passed through the specimen was measured, and the concrete permeability was classified according to the threshold values presented in Table 3-1. The rapid chloride permeability testing apparatus is shown in Figure 3-16.

Table 3-1: Rapid Chloride Permeability Classifications

Concrete Permeability	Charge Passed (Coulombs)
Very Low	< 1000
Low	1000 to 2000
Moderate	2000 to 4000
High	> 4000

Figure 3-16: Rapid chloride permeability testing apparatus.

3.6.4   Thermal Conductivity Testing

Thermal conductivity testing was performed during a 4-month period between August 2015 and November 2015, at which point the cylinders were considered to be representative of their long-term condition, using a needle-type sensor on one cylinder of each concrete type measuring 6 in. in diameter and 12 in. in height. Each cylinder was tested in different conditions, including wet, dry, low-temperature, and high-temperature conditions; low and high temperatures were determined from the minimum and maximum field temperatures, respectively, experienced by the pavement. To facilitate the testing, holes measuring 5/32 in. in diameter were drilled 2.4 in. deep into the center of both the top and bottom of each cylinder. The holes were filled with sufficient thermal lubricant to ensure full contact between the sensor needle and the surrounding concrete during testing. The needle was allowed to equilibrate in the hole for 3 minutes before beginning a test. After equilibration, a 10-minute test was performed, and the thermal conductivity and average concrete temperature during the test were recorded. Three

tests were performed in each of the two holes drilled into each cylinder, for a total of six tests per cylinder in each of the four conditions. Because the concrete temperature can change in the immediate vicinity of the needle during testing, tests were alternated between the typical and darkened concrete cylinders to allow the concrete to re-equilibrate.

The wet condition was that achieved after continuous curing in the fog room, and testing in this condition was performed in the fog room. After this testing was complete, the cylinders were allowed to air dry at room temperature for two weeks, which established the dry condition evaluated in this research. After being tested at room temperature, the cylinders were sealed in plastic bags to prevent further drying and to maintain a constant moisture content throughout the remaining tests. For the low-temperature condition, the sealed cylinders were placed in an environmental chamber set to 5°F and tested after a 72-hour equilibration period. Finally, for the high-temperature condition, the sealed cylinders were placed in an oven set to 150°F and tested after a 72-hour equilibration period. Thermal conductivity testing of a darkened concrete cylinder in the dry condition is shown in Figure 3-17.

3.6.5   Schmidt Rebound Hammer Testing

Schmidt rebound hammer tests were performed on the same cylinders used in thermal conductivity testing and in the same conditions, including wet, dry, low-temperature, and high-temperature conditions. Before the first test was performed, three locations were marked on both the top and the bottom of each cylinder, and one Schmidt rebound hammer test was performed at each of the marked locations, for a total of six tests per cylinder in each of the four conditions. Schmidt rebound hammer testing of a darkened concrete cylinder in the dry condition is shown in Figure 3-18.

27

Figure 3-17: Thermal conductivity testing.

Figure 3-18: Schmidt rebound hammer testing.

3.7 Summary

UDOT directed construction of a new 9-in.-thick concrete pavement, reinforced with dowels and tie bars, along 1000 West in Logan, Utah, during the summer of 2013. At the intersection of 1000 West and 1400 North, one section each of typical and darkened concrete pavement was placed on the west side, while two sections each of typical and darkened concrete pavement were placed on the east side. Both the typical and the darkened concrete pavement sections were instrumented with temperature and moisture sensors to enable monitoring of surface and subsurface temperatures and moisture contents on hourly intervals. At one typical and one darkened concrete pavement section on each side of the intersection, one location within a wheel path was selected for installation of sensors at the top and bottom of the concrete slab; measuring temperature and moisture at both the top and bottom of the concrete slabs allowed for computation of the temperature and moisture gradients at the selected locations. In addition to the sensors in the concrete, environmental sensors were also installed to measure ambient conditions, including air temperature, relative humidity, and precipitation. Each sensor cable was connected to a battery-powered data logger that was programmed to collect data from the sensors on an hourly basis and send the data to a remotely accessible database through a daily cellular transmission.

After the temperature and moisture sensors and the thermocouple wires were all installed, either typical or darkened concrete was placed in each section. The researchers cast 10 4-in. by 8-in. cylinders of each type of concrete on each side of the intersection during placement. In addition, the researchers cast two 6-in. by 12-in. cylinders of each type of concrete on the east side.

Following construction of the pavement sections, the researchers returned to the site for additional testing in November 2013, February 2014, June 2014, and September 2014. During each site visit, they performed testing at four or five different times during a given 24-hour period. Procedures related to field testing included infrared thermography, thermocouple readings, sensor data collection, and roughness surveys. Elevation surveys and albedo measurements were also performed to further characterize the site. Elevations were measured around the perimeter of the main lanes in each section at 10-ft intervals in the longitudinal direction and at 5-ft intervals in the transverse direction. Albedo measurements were measured using a pyranometer with the pavement in both dry and wet conditions.

At each testing time, the researchers documented surface temperatures using infrared thermography, recorded the subsurface temperatures as measured using the thermocouple wires and a thermocouple reader, and performed pavement roughness surveys using a roadway profiler in the wheel paths of each section. To obtain the sensor data, including pavement temperature and moisture and air temperature, relative humidity, and precipitation, the researchers remotely downloaded data from the data loggers approximately bi-weekly.

Procedures related to laboratory testing included elastic modulus, compressive strength, rapid chloride permeability, thermal conductivity, and Schmidt rebound hammer testing of cylinders prepared from typical and darkened concrete. As an assessment of the elastic modulus of the typical and darkened concrete, non-destructive free-free resonant tests were conducted on cylinders measuring 4 in. in diameter and 8 in. in height at 7 days, 28 days, 6 months, and 1 year. Compressive strength tests were performed at 7 days, 28 days, 6 months, and 1 year on the same cylinders used in elastic modulus testing. Rapid chloride permeability testing was performed on two cylinders of each concrete type measuring 4 in. in diameter and 8 in. in height at 28 days, 6

months, and 1 year. Test samples were cut to a thickness of 2 in. from the middle of the

cylinders using a masonry saw. Thermal conductivity testing was performed during a 4-month

period between August 2015 and November 2015 using a needle-type sensor on one cylinder of

each concrete type measuring 6 in. in diameter and 12 in. in height. Each cylinder was tested in

different conditions, including wet, dry, low-temperature, and high-temperature conditions; low

and high temperatures were determined from the minimum and maximum field temperatures,

respectively, experienced by the pavement. Schmidt rebound hammer tests were performed on

the same cylinders used in thermal conductivity testing and in the same conditions.

4   RESULTS

4.1   Overview

The following sections describe the results of field and laboratory testing. All results

presented in this chapter are limited in their application to the material types, pavement designs,

construction techniques, environmental conditions, and trafficking levels associated with this

study.

4.2   Field Testing

Results related to field testing include elevation surveys, albedo measurements, infrared

thermography, thermocouple readings, sensor data collection, and roughness surveys. Tables

and figures providing relevant supporting data for the analyses presented in this section are given

in Appendix A.

4.2.1   Elevation Surveys

Elevation surveys were performed to measure both the average transverse and

longitudinal slopes at each test site. Figure 4-1 shows the average transverse slopes for all sites

along the east and west sides of the main lanes and the average longitudinal slopes for all sites

along the north and south sides of the main lanes in each section. For the transverse surveys, the

slopes were calculated with respect to the elevation of the crown at each site; therefore, a

positive transverse slope indicates that the pavement sloped upward toward the outer edge of the
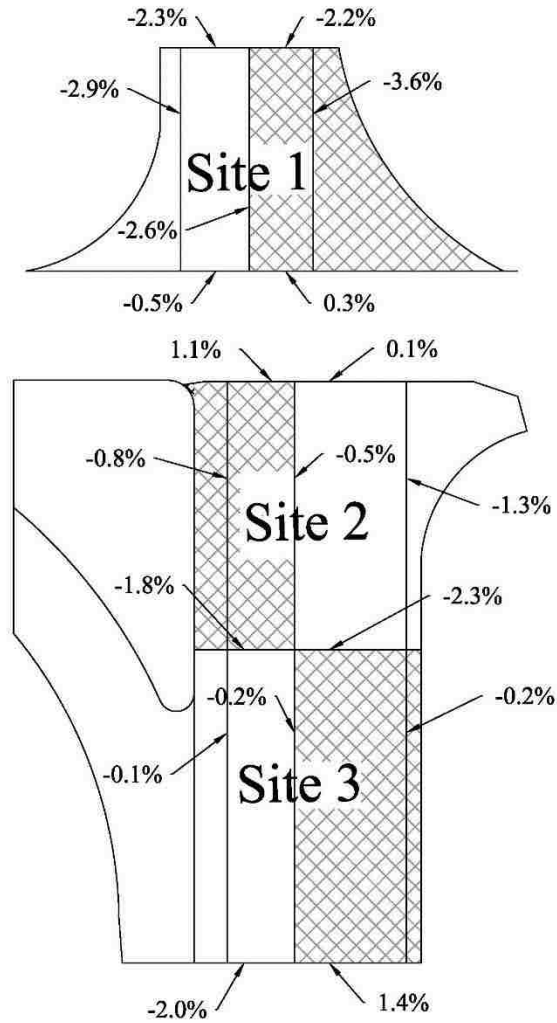
Figure 4-1: Transverse and longitudinal slopes.

section, while a negative transverse slope indicates that the pavement sloped downward toward the outer edge of the section. For the longitudinal surveys, the slopes were calculated with respect to the edge of the pavement closest to the intersection, meaning the east edge of site 1 and the west edges of sites 2 and 3; therefore, a negative longitudinal slope indicates that the pavement sloped downward away from the intersection. The variable slope measurements suggest that not all of the sections were planar and that not all of the sections experienced consistent solar radiation intensity during all seasons due to the non-zero zenith angle in this

region. The occurrence of varying transverse and longitudinal pavement slopes ensured that the data were representative of typical roads.

4.2.2   Albedo Measurements

The results of albedo testing were averaged by section and condition as shown in Figure 4-2. The average albedo for the darkened concrete pavement was lower than the average albedo of the typical concrete pavement by 0.099 to 0.103, or 33 to 34 percent, and was higher than the average albedo of the asphalt pavement by 0.041 to 0.054, or 26 to 34 percent, depending on the pavement condition. Thus, while the use of the iron oxide pigment in the darkened concrete was successful in achieving a lower albedo than that of the typical concrete pavement, the albedo was still higher than that of the adjacent asphalt pavement at the time of testing.
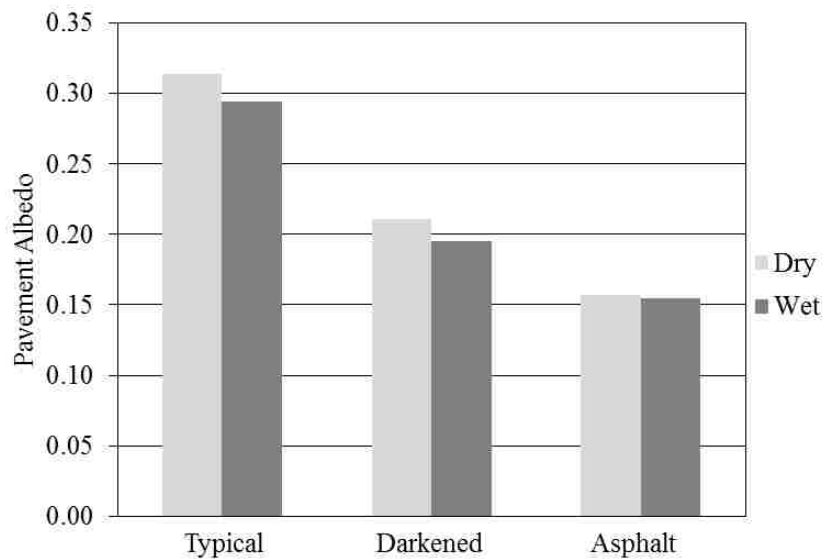

Figure 4-2: Pavement albedo.

4.2.3 Infrared Thermography

Surface pavement temperatures were calculated from the infrared images by averaging the temperature measurements at the approximate locations of the four thermocouples in each instrumented section. As shown in Figure 4-3, measurements in each section were made at four or five different times of day in each season, including fall, winter, spring, and summer. Representative infrared images and temperature measurements corresponding to specific testing times are given in Appendix A.

When considered over the entire monitoring period, the average surface temperatures of the darkened pavement were higher than those of the typical pavement by 3.3°F, or 5.0 percent. The range of surface temperatures experienced by the pavement in a given day is usually larger during spring and summer than during fall and winter.
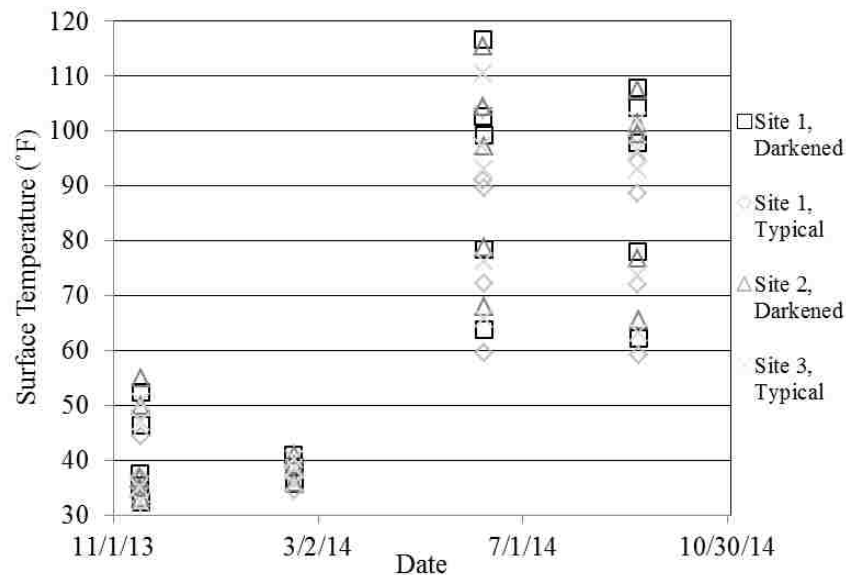

Figure 4-3: Surface temperatures measured using infrared thermography.

Figures 4-4 and 4-5 show correlations between air temperature readings and surface temperature readings. As explained previously, the sensors and thermocouples for sites 2 and 3 were placed only in the south side of the roadway, which consisted of darkened pavement in site 2 and typical pavement in site 3 as shown in Figure 3-3. A strong positive correlation exists between the air temperature and the surface pavement temperatures, as shown in Figure 4-4. Differences in surface pavement temperatures between the typical and darkened concrete sections were calculated by subtracting the value of the typical concrete from the value of the darkened concrete. Figure 4-5 shows that the difference between the surface temperatures of the darkened and typical pavements decreases as the air temperature decreases. Indeed, the results of a simple linear regression suggest that, when the air temperature is 32°F, the surface temperature of the darkened concrete is just 0.2°F higher than that of the typical concrete, and the difference is expected to be 0°F when the air temperature is 30.5°F. Therefore, the darkened
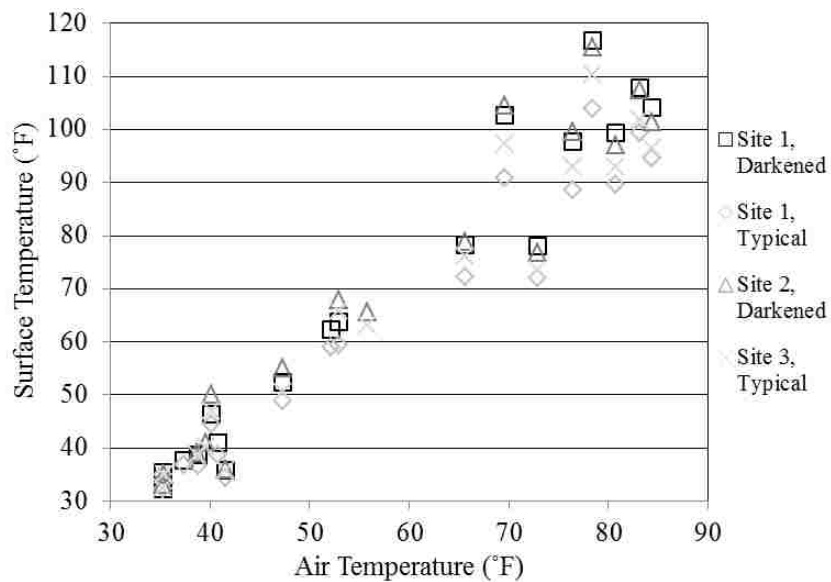

Figure 4-4: Air temperature from data logger readings compared to pavement surface temperatures from infrared thermography.
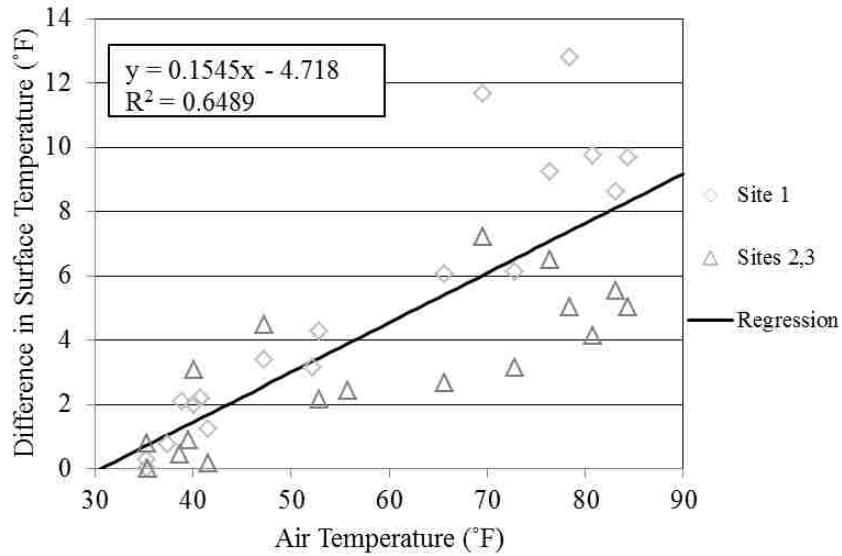
Figure 4-5: Air temperature from data logger readings compared to differences in pavement surface temperatures from infrared thermography.

pavement is unlikely to melt snow and ice faster than the typical pavement for conditions similar to those in this research.

4.2.4 Thermocouple Readings

Subsurface pavement temperatures, shown in Figure 4-6, were calculated using the average of the four thermocouple readings from each site. When considered over the entire monitoring period, the average subsurface temperatures of the darkened pavement were higher than those of the typical pavement by 3.1°F, or 4.9 percent. Similar to the surface temperature, the range of subsurface temperatures experienced by the pavement in a given day is usually larger during spring and summer than during fall and winter; however, variations in subsurface temperature within a given day were much less than the variations in surface temperature during the same day. Temperature measurements corresponding to specific testing times are given in Appendix A.

Figures 4-7 and 4-8 show correlations between air temperature readings and subsurface temperature readings. A strong positive correlation exists between the air temperature and the subsurface pavement temperatures, as shown in Figure 4-7. Differences in subsurface pavement
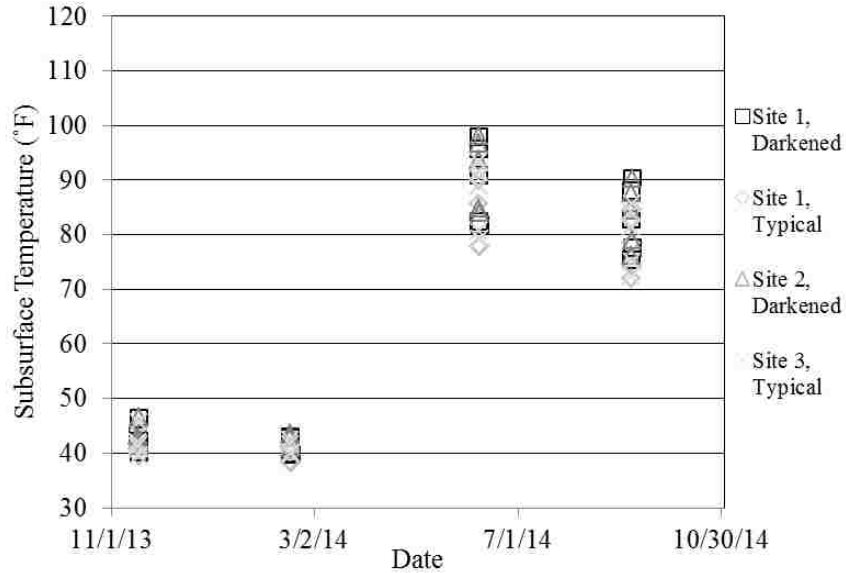

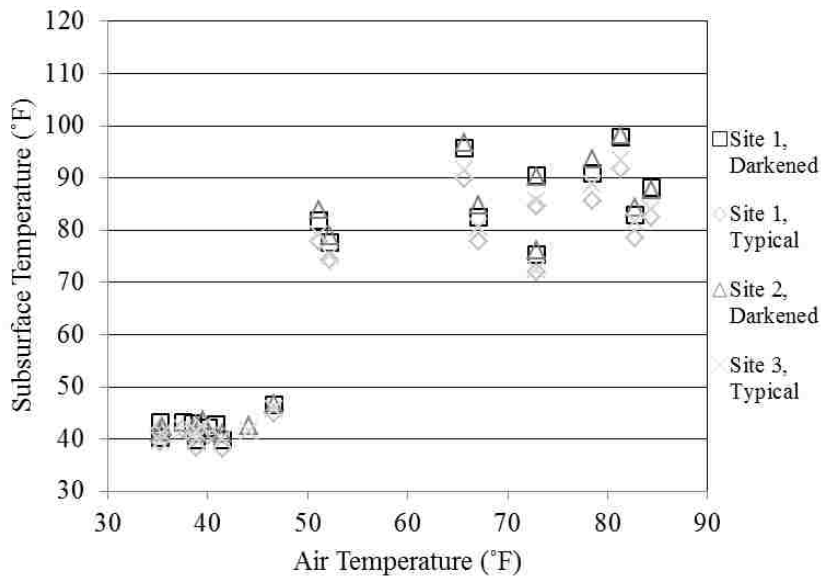**Figure 4-6: Subsurface temperatures measured using thermocouples.**

Figure 4-7: Air temperature from data logger readings compared to pavement subsurface temperature from thermocouple readings.
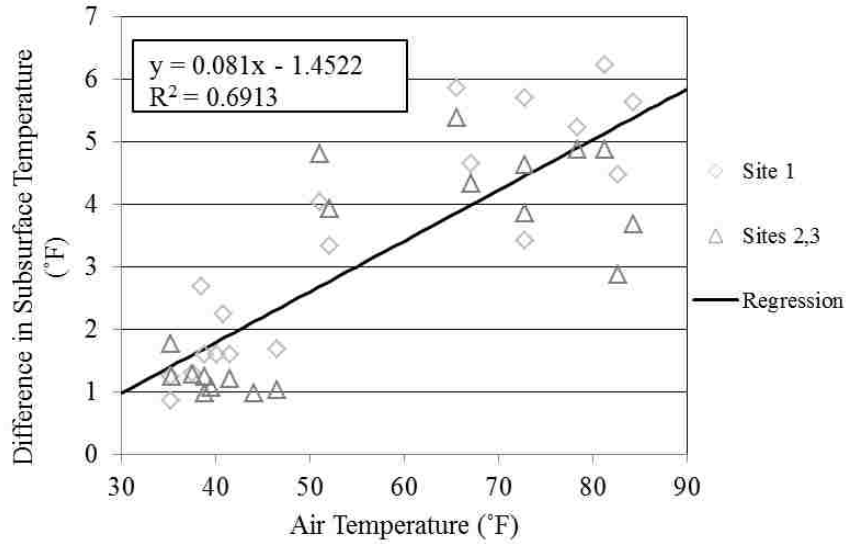
38

Figure 4-8: Air temperature from data logger readings compared to differences in pavement subsurface temperatures from thermocouple readings.

temperatures between the typical and darkened concrete sections were calculated by subtracting

the value of the typical concrete from the value of the darkened concrete. Figure 4-8 shows that

the difference between the subsurface temperatures of the darkened and typical pavements also

decreases as the air temperature decreases. In this case, the results of a simple linear regression

suggest that, when the air temperature is 32°F, the subsurface temperature of the darkened

concrete is 1.1°F higher than that of the typical concrete, and the difference is expected to be 0°F

when the air temperature is 17.9°F. Therefore, the darkened pavement is unlikely to provide

significantly greater frost protection to subsurface layers and buried utilities during winter for

conditions similar to those in this research.

4.2.5   Sensor Data

Pavement temperature and moisture data collected from the upper and lower sensors

embedded in the concrete are presented graphically in Appendix A. (The embedded sensors had

the capability of measuring pavement electrical conductivity in addition to pavement temperature and moisture, and those data are also presented graphically in Appendix A.)

Figure 4-9 shows temperature gradients determined using the temperature sensors. Temperature gradients were calculated from sensor readings obtained through the data loggers by subtracting the values measured at a given time by the upper temperature sensor from the values measured at the same time by the lower temperature sensor and dividing by the vertical distance between the sensors. When considered over the entire monitoring period, the average pavement temperature gradient of the darkened pavement was lower than that of the typical pavement at site 1 by 0.411 °F/in., or 796 percent, and higher than that of the typical pavement at sites 2 and 3 by 0.535 °F/in., or 735 percent. The lower sensor in the typical concrete at site 3 apparently malfunctioned beginning in May 2014, and temperature and moisture data from that sensor are consequently excluded beyond that date.

Figure 4-10 shows moisture gradients determined using the moisture sensors. Moisture gradients were calculated from sensor readings obtained through the data loggers by subtracting the values measured at a given time by the upper moisture sensor from the values measured at the same time by the lower moisture sensor and dividing by the vertical distance between the sensors. When considered over the entire monitoring period, the average pavement moisture gradient of the darkened pavement was higher than that of the typical pavement at site 1 by 0.041 %/in., or 17 percent, and lower than that of the typical pavement at sites 2 and 3 by 0.859 %/in., or 127 percent. (Due to the high ion concentrations typical of pore water in concrete, the moisture content recorded by the temperature and moisture sensors may be affected by the temperature of the concrete surrounding the sensors).
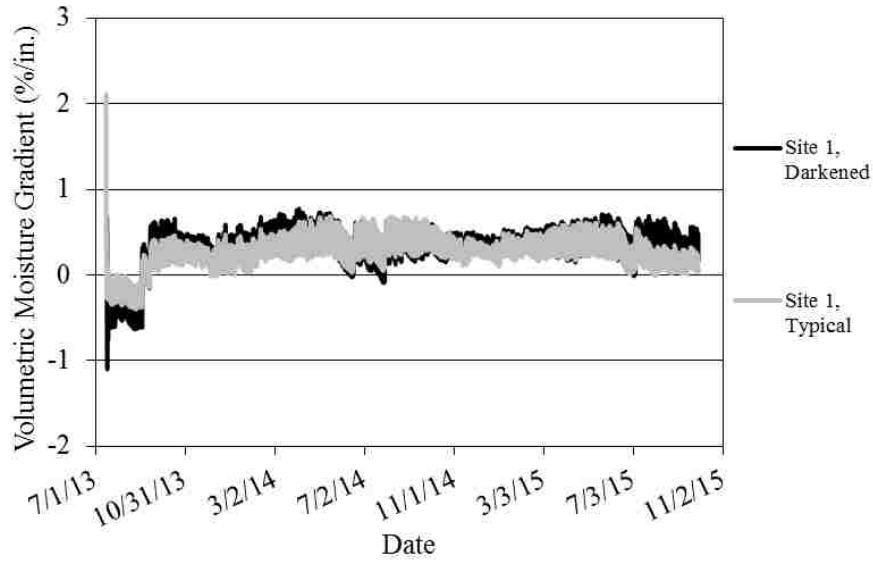
40
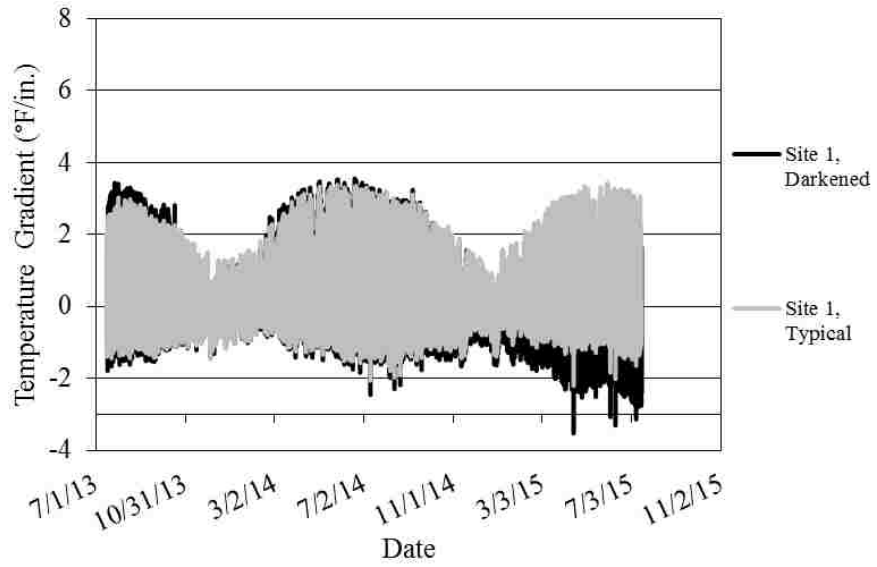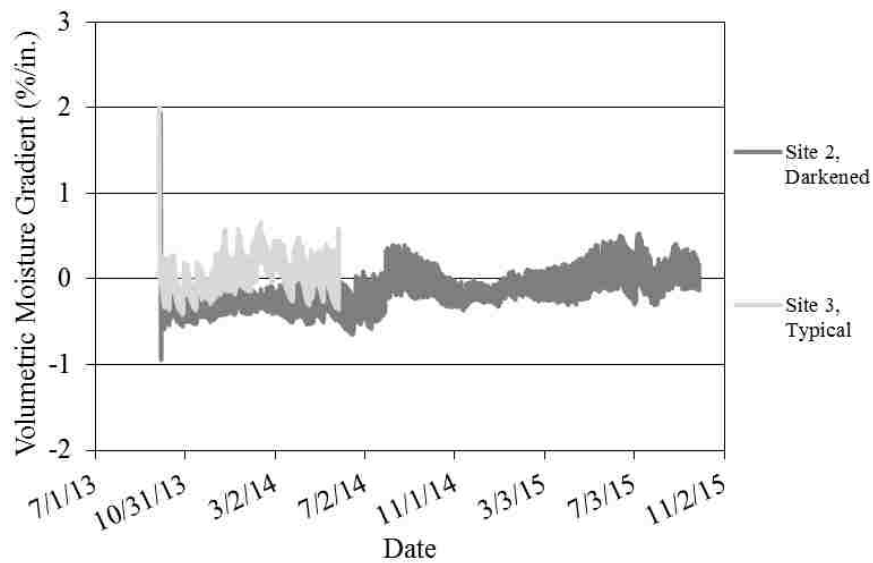
(a)
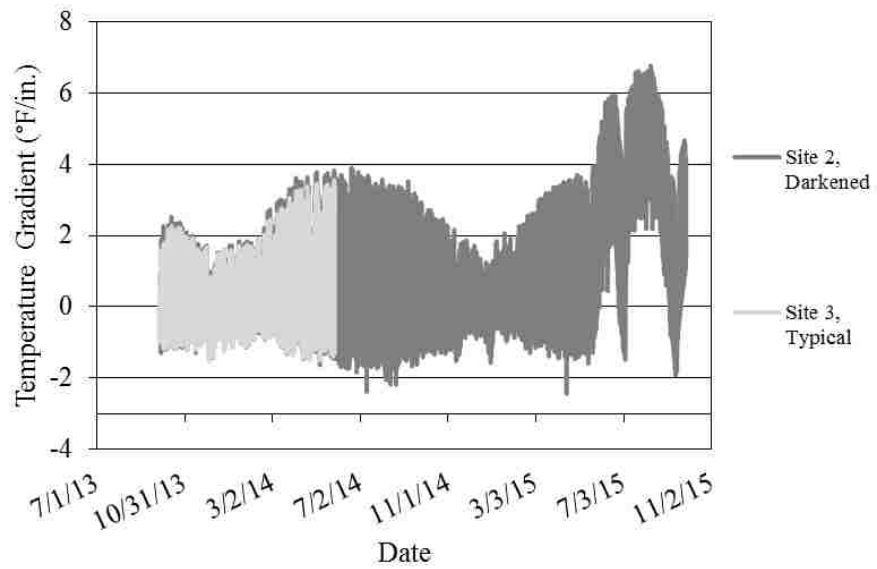
(b)

Figure 4-9: Temperature gradients for (a) site 1 and (b) sites 2 and 3.

(a)

(b)

Figure 4-10: Moisture gradients for (a) site 1 and (b) sites 2 and 3.

4.2.6 Roughness

Figures 4-11 and 4-12 show pavement roughness for the left wheel path (LWP) and right wheel path (RWP) of all typical and darkened concrete sections, respectively. The roughness measurements for the typical pavement exhibit much more daily variability than seasonal
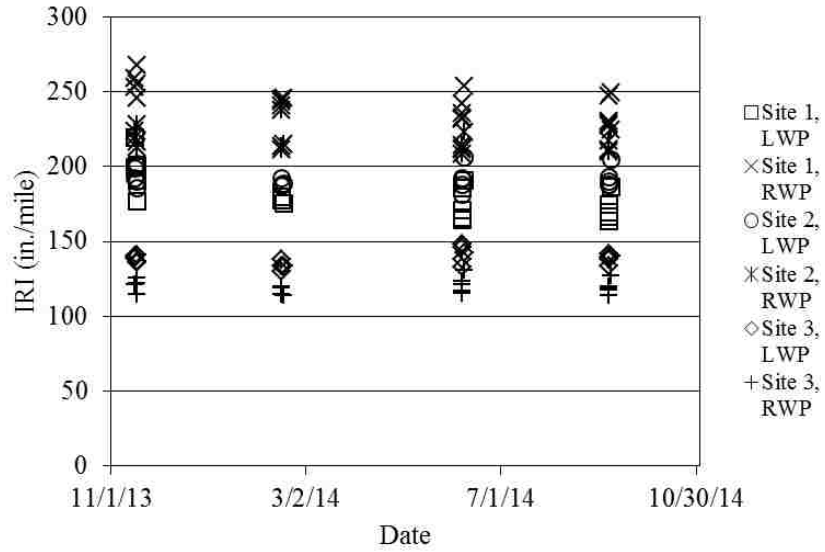
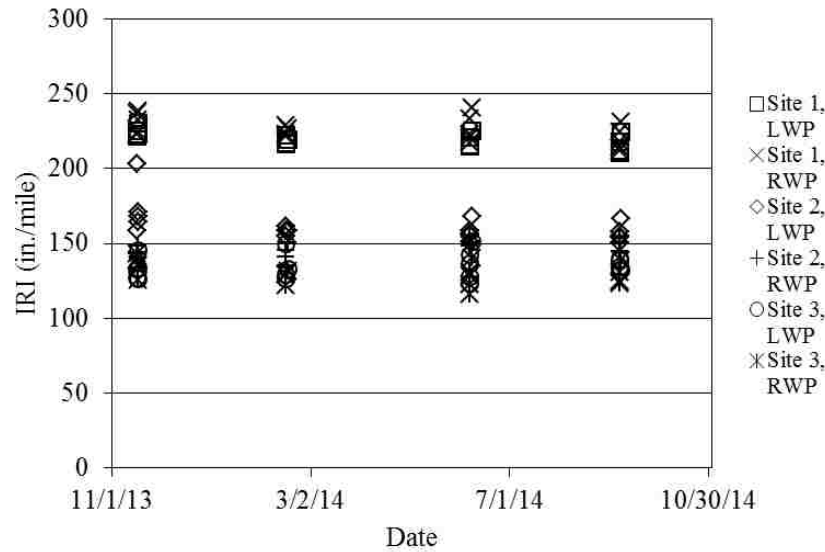**Figure 4-11: Roughness for all typical concrete sections.**

Figure 4-12: Roughness for all darkened concrete sections.

variability. The roughness measurements for the darkened pavement also exhibit more daily variability than seasonal variability but less overall variability than that of the typical pavement. Differences in roughness between wheel paths are likely a result of variation in built-in roughness.

Figures 4-13 and 4-14 show pavement roughness plotted against temperature gradient for all wheel paths of all typical and darkened concrete sections, respectively. Pavement temperature gradient does not appear to be correlated to roughness for either the typical pavement or the darkened pavement. Indeed, measurable curling and warping do not appear to be occurring at this site; the combination of joint spacing, slab thickness, steel reinforcement, and concrete strength at this site apparently minimized the occurrence of curling and warping.

Figures 4-15 and 4-16 show pavement roughness plotted against moisture gradient for all typical and darkened concrete sections, respectively. Pavement moisture gradient does not appear to be correlated to roughness for either the typical pavement or the darkened pavement. This lack of correlation may also be associated with the combination of joint spacing, slab thickness, steel reinforcement, and concrete strength at this site.
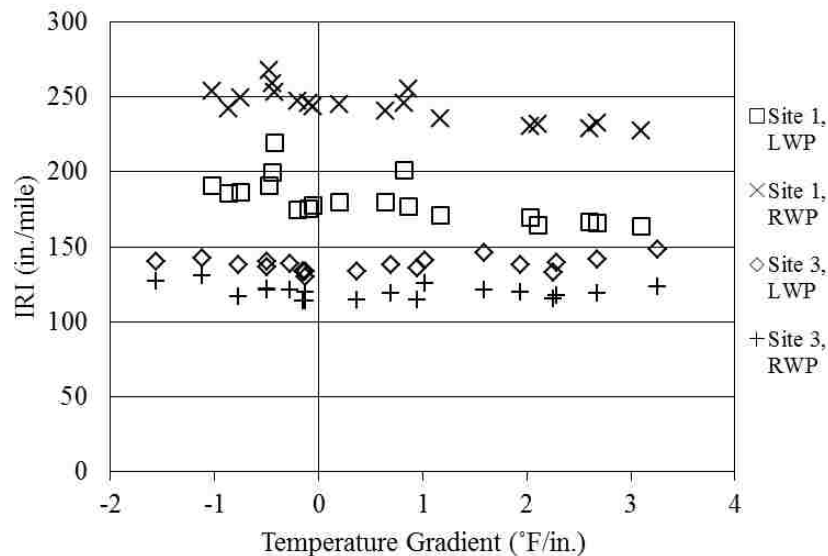

Figure 4-13: Roughness and temperature gradient for all typical concrete sections.
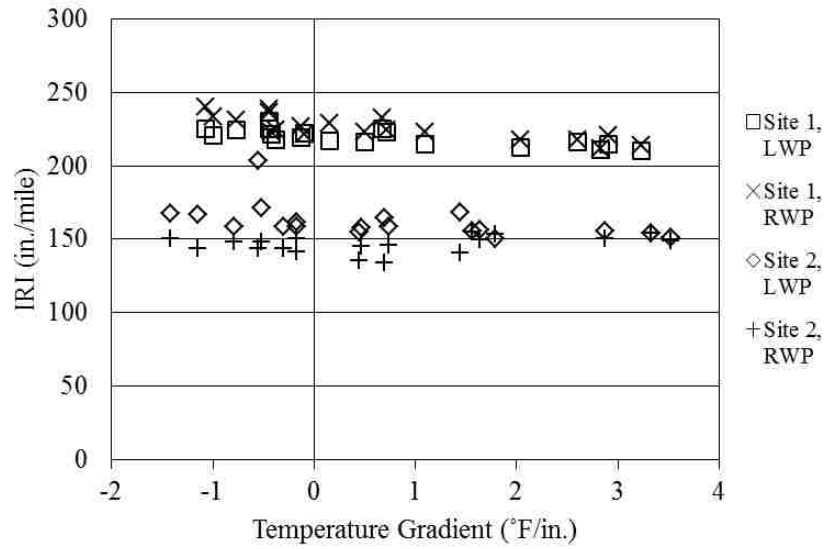
Figure 4-14: Roughness and temperature gradient for all darkened concrete sections.
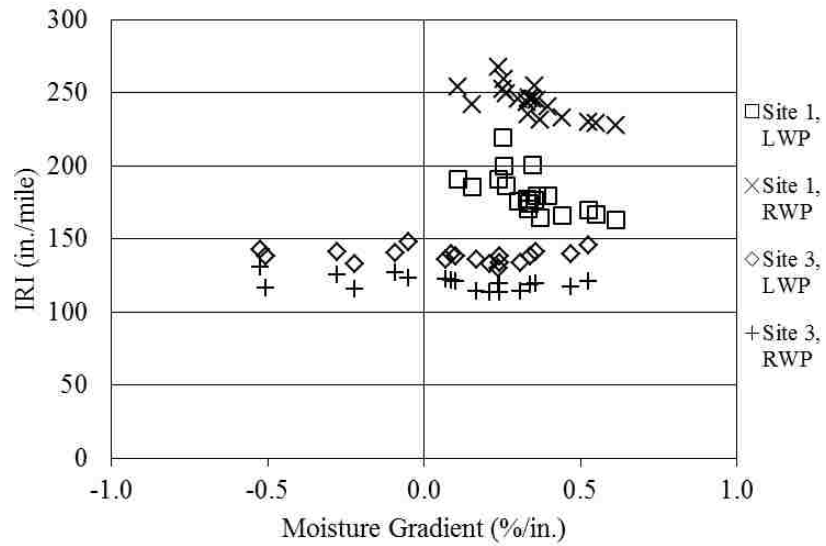

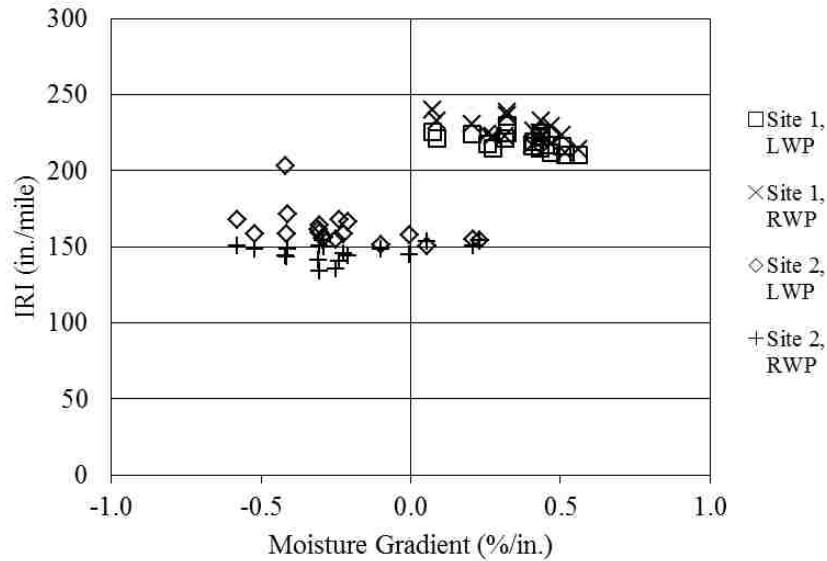**Figure 4-15: Roughness and moisture gradient for all typical concrete sections.**

45

Figure 4-16: Roughness and moisture gradient for all darkened concrete sections.

4.3 Laboratory Testing

Results related to laboratory testing include elastic modulus, compressive strength, rapid chloride permeability, Schmidt rebound hammer, and thermal conductivity of cylinders prepared from typical and darkened concrete. Tables and figures providing relevant supporting data for the analyses presented in this section are given in Appendix B.

4.3.1 Elastic Modulus Testing

Figure 4-17 shows average concrete elastic modulus values. Specific cylinder length, diameter, weight, density, frequency, and elastic modulus values are given in Appendix B. On average, the darkened concrete was stiffer than the typical concrete by 220 ksi, or 10.3 percent, at 1 year.
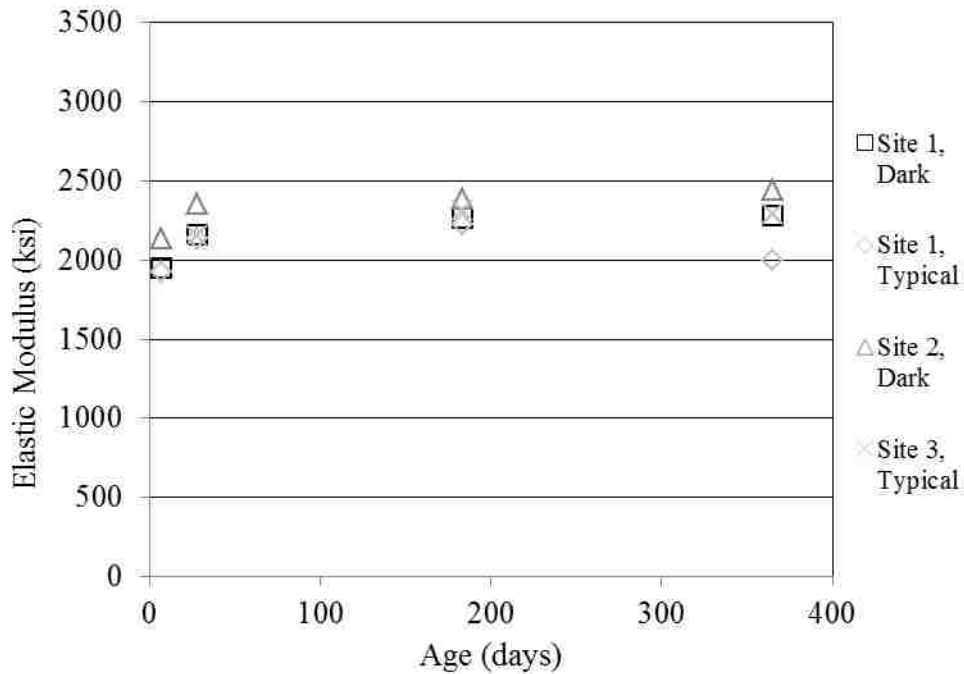
46

Figure 4-17: Average concrete elastic modulus.

4.3.2   Compressive Strength Testing

Figure 4-18 shows average concrete compressive strengths. Specific cylinder compressive strengths are given in Appendix B. As expected, the concrete compressive strength increases over time. On average, the darkened concrete was stronger than the typical concrete by 1017 psi, or 17.2 percent, at 1 year.

4.3.3   Rapid Chloride Permeability Testing

Figure 4-19 shows average rapid chloride permeability values. Specific sample rapid chloride permeability values and classifications are given in Appendix B. As expected, chloride permeability decreases over time. At 28 days, both concrete types were classified as having "low" permeability, while at all testing times beyond 28 days, both concrete types were classified
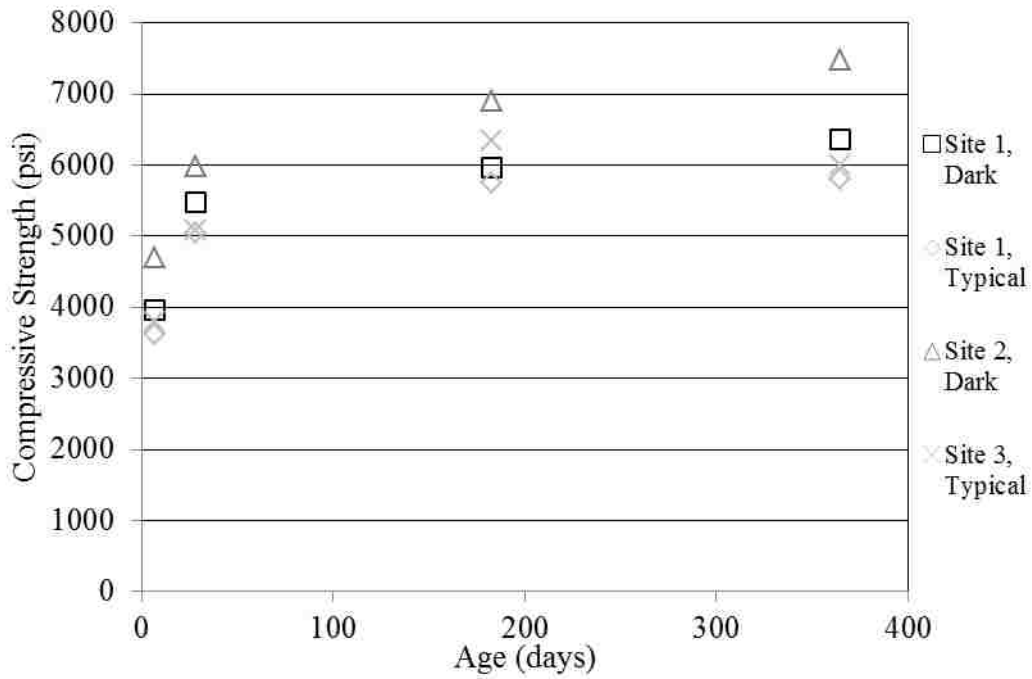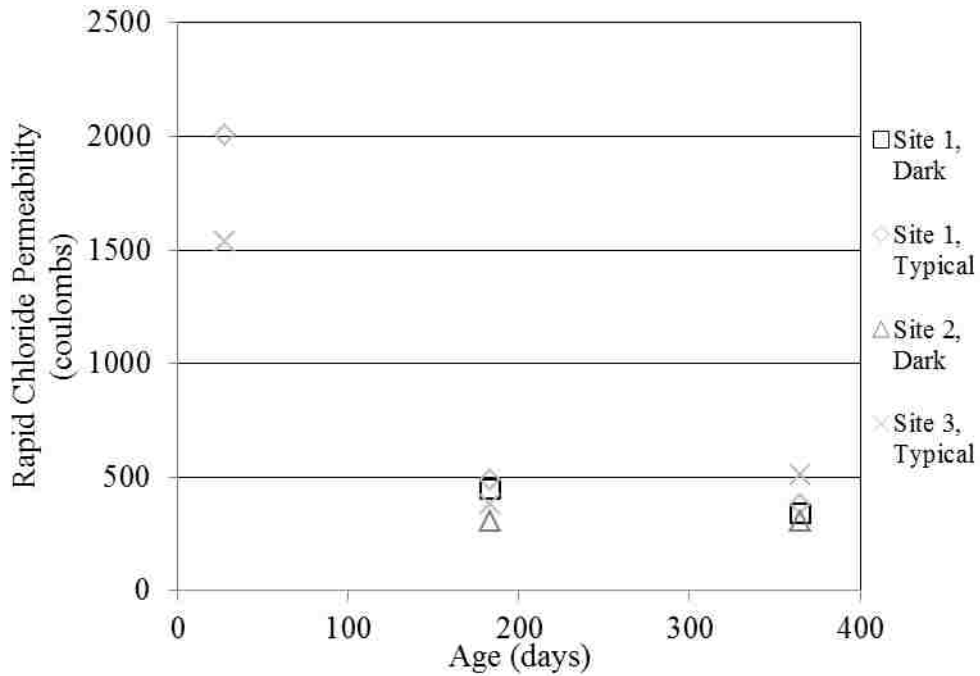
Figure 4-18: Concrete compressive strength.

Figure 4-19: Rapid chloride permeability.

as having "very low" permeability. On average, the darkened concrete was less permeable than the typical concrete by 119 coulombs, or 26.8 percent, at 1 year.

4.3.4   Thermal Conductivity Testing

Figure 4-20 shows average thermal conductivity values. Specific thermal conductivity values and the temperatures at which those values were measured are given in Appendix B. On average, the thermal conductivity of the darkened concrete was higher than that of the typical concrete by 0.272 W/m*K, or 7.7 percent.
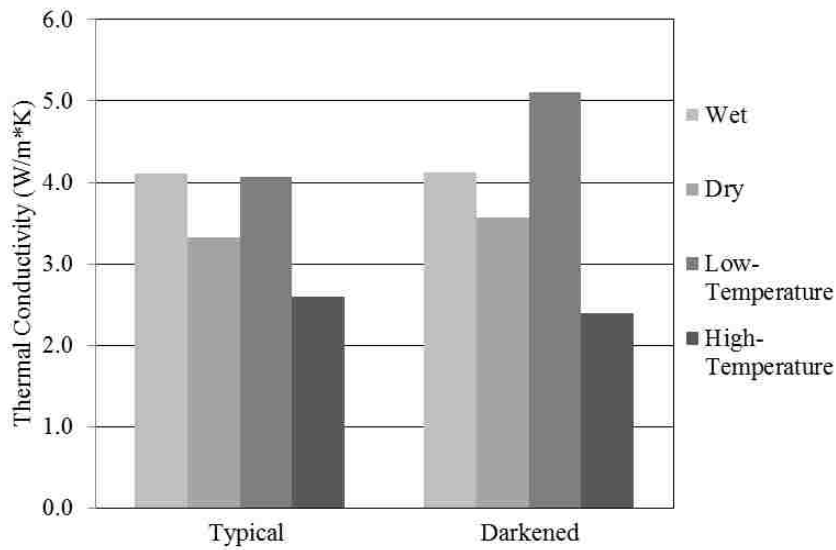

Figure 4-20: Average thermal conductivity.

4.3.5   Schmidt Rebound Hammer Testing

Figure 4-21 shows the average Schmidt rebound numbers. On average, the Schmidt rebound number of the darkened concrete was higher than that of the typical concrete by 4.9, or 13.9 percent. This result is consistent with the compressive strength test results presented earlier.
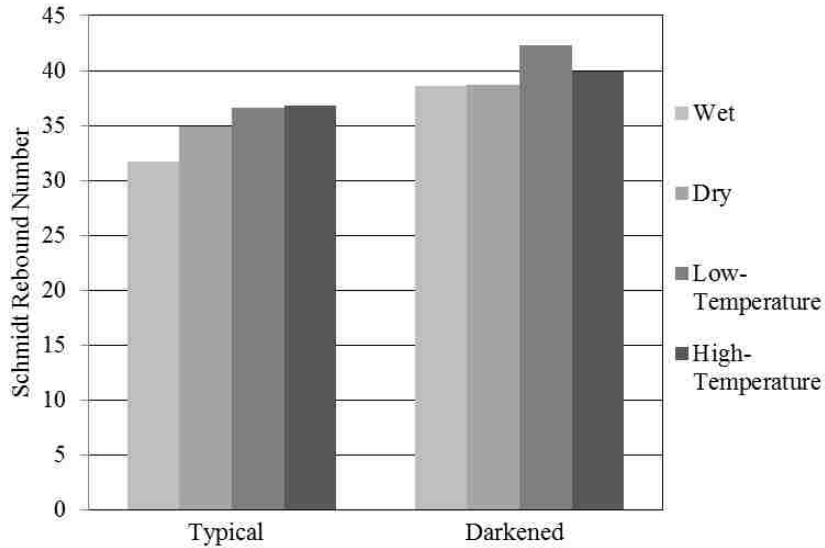
Figure 4-21: Average Schmidt rebound numbers.

4.4 Summary

Results related to field testing include elevation surveys, albedo measurements, infrared thermography, thermocouple readings, sensor data collection, and roughness surveys. Elevation surveys were performed to measure both the average transverse and longitudinal slopes at each test site. The variable slope measurements suggest that not all of the sections were planar and that not all of the sections experienced consistent solar radiation intensity during all seasons due to the non-zero zenith angle in this region. The average albedo for the darkened concrete pavement was lower than the average albedo of the typical concrete pavement by 33 to 34 percent and was higher than the average albedo of the asphalt pavement by 26 to 34 percent, depending on the pavement condition. Thus, while the use of the iron oxide pigment in the darkened concrete was successful in achieving a lower albedo than that of the typical concrete pavement, the albedo was still higher than that of the adjacent asphalt pavement at the time of testing.

When considered over the entire monitoring period, the average surface temperatures of the darkened pavement were higher than those of the typical pavement by 3.3°F, and the average subsurface temperatures of the darkened pavement were higher than those of the typical pavement by 3.1°F. A strong positive correlation exists between the air temperature and both the surface and the subsurface pavement temperatures. The difference between the surface temperatures of the darkened and typical pavements decreases as the air temperature decreases. Indeed, the results of a simple linear regression suggest that, when the air temperature is 32°F, the surface temperature of the darkened concrete is just 0.2°F higher than that of the typical concrete, and the difference is expected to be 0°F when the air temperature is 30.5°F. Therefore, the darkened pavement is unlikely to melt snow and ice faster than the typical pavement for conditions similar to those in this research. The difference between the subsurface temperatures of the darkened and typical pavements also decreases as the air temperature decreases. In this case, the results of a simple linear regression suggest that, when the air temperature is 32°F, the subsurface temperature of the darkened concrete is 1.1°F higher than that of the typical concrete, and the difference is expected to be 0°F when the air temperature is 17.9°F. Therefore, the darkened pavement is unlikely to provide significantly greater frost protection to subsurface layers and buried utilities during winter for conditions similar to those in this research.

When considered over the entire monitoring period, the average pavement temperature gradient of the darkened pavement was lower than that of the typical pavement at site 1 by 796 percent and higher than that of the typical pavement at sites 2 and 3 by 735 percent, and the average pavement moisture gradient of the darkened pavement was higher than that of the typical pavement at site 1 by 17 percent and lower than that of the typical pavement at sites 2 and 3 by 127 percent.

The roughness measurements for the typical pavement exhibit much more daily variability than seasonal variability. The roughness measurements for the darkened pavement also exhibit more daily variability than seasonal variability but less overall variability than that of the typical pavement. Neither pavement temperature gradient nor moisture gradient appears to be correlated to roughness for either the typical pavement or the darkened pavement. Measurable curling and warping do not appear to be occurring at this site; the combination of joint spacing, slab thickness, steel reinforcement, and concrete strength at this site apparently minimized the occurrence of curling and warping.

Results related to laboratory testing include elastic modulus, compressive strength, rapid chloride permeability, Schmidt rebound hammer, and thermal conductivity of cylinders prepared from typical and darkened concrete. On average, the darkened concrete was stiffer than the typical concrete by 10.3 percent, stronger than the typical concrete by 17.2 percent, and less permeable than the typical concrete by 26.8 percent at 1 year. On average, the thermal conductivity of the darkened concrete was higher than that of the typical concrete by 7.7 percent, and the Schmidt rebound number of the darkened concrete was higher than that of the typical concrete by 13.9 percent.

5 CONCLUSION

5.1 Summary

While portland cement concrete pavement offers a durable surface and long service life when designed and constructed properly, concrete pavement sections can require more expensive winter maintenance treatments to clear snow and ice in cold regions than asphalt pavement sections. One method of potentially reducing winter maintenance costs is darkening the concrete pavement; however, little research exists on the use of this method. Darkening the concrete reduces its albedo, or whiteness, and would therefore be expected to change its thermal behavior.

Darkened concrete should promote higher pavement surface temperatures through increased absorption of radiation energy from the sun. Higher surface temperatures may also lead to higher moisture gradients through the depth of the slab, causing greater slab warping. Both curling and warping of concrete slabs can lead to a rougher pavement surface; roughness is an important factor in pavement serviceability assessment, as it has a large impact on the traveling public.

The objectives of this research were to 1) investigate the effects of lower concrete albedo on the thermal behavior of concrete pavement by directly comparing temperatures and moisture contents of typical and darkened concrete pavements and 2) investigate changes in roughness of both typical and darkened concrete pavements as a result of changes in temperature and moisture

gradients. The scope of the research included instrumentation, testing, and analysis of typical and darkened concrete pavements constructed in northern Utah.

UDOT directed construction of a new 9-in.-thick concrete pavement, reinforced with dowels and tie bars, along 1000 West in Logan, Utah, during the summer of 2013. At the intersection of 1000 West and 1400 North, one section each of typical and darkened concrete pavement was placed on the west side, while two sections each of typical and darkened concrete pavement were placed on the east side. Both the typical and the darkened concrete pavement sections were instrumented with temperature and moisture sensors to enable monitoring of surface and subsurface temperatures and moisture contents on hourly intervals. At one typical and one darkened concrete pavement section on each side of the intersection, one location within a wheel path was selected for installation of sensors at the top and bottom of the concrete slab; measuring temperature and moisture at both the top and bottom of the concrete slabs allowed for computation of the temperature and moisture gradients at the selected locations. In addition to the sensors in the concrete, environmental sensors were also installed to measure ambient conditions, including air temperature, relative humidity, and precipitation. Each sensor cable was connected to a battery-powered data logger that was programmed to collect data from the sensors on an hourly basis and send the data to a remotely accessible database through a daily cellular transmission.

After the temperature and moisture sensors and the thermocouple wires were all installed, either typical or darkened concrete was placed in each section. The researchers cast 10 4-in. by 8-in. cylinders of each type of concrete on each side of the intersection during placement. In addition, the researchers cast two 6-in. by 12-in. cylinders of each type of concrete on the east side.

Following construction of the pavement sections, the researchers returned to the site for additional testing in November 2013, February 2014, June 2014, and September 2014. During each site visit, they performed testing at four or five different times during a given 24-hour period. Procedures related to field testing included infrared thermography, thermocouple readings, sensor data collection, and roughness surveys. Elevation surveys and albedo measurements were also performed to further characterize the site. Elevations were measured around the perimeter of the main lanes in each section at 10-ft intervals in the longitudinal direction and at 5-ft intervals in the transverse direction. Albedo measurements were measured using a pyranometer with the pavement in both dry and wet conditions.

At each testing time, the researchers documented surface temperatures using infrared thermography, recorded the subsurface temperatures as measured using the thermocouple wires and a thermocouple reader, and performed pavement roughness surveys using a roadway profiler in the wheel paths of each section. To obtain the sensor data, including pavement temperature and moisture and air temperature, relative humidity, and precipitation, the researchers remotely downloaded data from the data loggers approximately bi-weekly.

Procedures related to laboratory testing included elastic modulus, compressive strength, rapid chloride permeability, thermal conductivity, and Schmidt rebound hammer testing of cylinders prepared from typical and darkened concrete. As an assessment of the elastic modulus of the typical and darkened concrete, non-destructive free-free resonant tests were conducted on cylinders measuring 4 in. in diameter and 8 in. in height at 7 days, 28 days, 6 months, and 1 year. Compressive strength tests were performed at 7 days, 28 days, 6 months, and 1 year on the same cylinders used in elastic modulus testing. Rapid chloride permeability testing was performed on two cylinders of each concrete type measuring 4 in. in diameter and 8 in. in height at 28 days, 6

months, and 1 year. Test samples were cut to a thickness of 2 in. from the middle of the cylinders using a masonry saw. Thermal conductivity testing was performed during a 4-month period between August 2015 and November 2015 using a needle-type sensor on one cylinder of each concrete type measuring 6 in. in diameter and 12 in. in height. Each cylinder was tested in different conditions, including wet, dry, low-temperature, and high-temperature conditions; low and high temperatures were determined from the minimum and maximum field temperatures, respectively, experienced by the pavement. Schmidt rebound hammer tests were performed on the same cylinders used in thermal conductivity testing and in the same conditions.

5.2   Findings

Results related to field testing include elevation surveys, albedo measurements, infrared thermography, thermocouple readings, sensor data collection, and roughness surveys. Elevation surveys were performed to measure both the average transverse and longitudinal slopes at each test site. The variable slope measurements suggest that not all of the sections were planar and that not all of the sections experienced consistent solar radiation intensity during all seasons due to the non-zero zenith angle in this region. The average albedo for the darkened concrete pavement was lower than the average albedo of the typical concrete pavement by 33 to 34 percent and was higher than the average albedo of the asphalt pavement by 26 to 34 percent, depending on the pavement condition. Thus, while the use of the iron oxide pigment in the darkened concrete was successful in achieving a lower albedo than that of the typical concrete pavement, the albedo was still higher than that of the adjacent asphalt pavement at the time of testing.

When considered over the entire monitoring period, the average surface temperatures of the darkened pavement were higher than those of the typical pavement by 3.3°F, and the average subsurface temperatures of the darkened pavement were higher than those of the typical pavement by 3.1°F. A strong positive correlation exists between the air temperature and both the surface and the subsurface pavement temperatures. The difference between the surface temperatures of the darkened and typical pavements decreases as the air temperature decreases. Indeed, the results of a simple linear regression suggest that, when the air temperature is 32°F, the surface temperature of the darkened concrete is just 0.2°F higher than that of the typical concrete, and the difference is expected to be 0°F when the air temperature is 30.5°F. Therefore, the darkened pavement is unlikely to melt snow and ice faster than the typical pavement for conditions similar to those in this research. The difference between the subsurface temperatures of the darkened and typical pavements also decreases as the air temperature decreases. In this case, the results of a simple linear regression suggest that, when the air temperature is 32°F, the subsurface temperature of the darkened concrete is 1.1°F higher than that of the typical concrete, and the difference is expected to be 0°F when the air temperature is 17.9°F. Therefore, the darkened pavement is unlikely to provide significantly greater frost protection to subsurface layers and buried utilities during winter for conditions similar to those in this research.

When considered over the entire monitoring period, the average pavement temperature gradient of the darkened pavement was lower than that of the typical pavement at site 1 by 796 percent and higher than that of the typical pavement at sites 2 and 3 by 735 percent, and the average pavement moisture gradient of the darkened pavement was higher than that of the typical pavement at site 1 by 17 percent and lower than that of the typical pavement at sites 2 and 3 by 127 percent.

The roughness measurements for the typical pavement exhibit much more daily variability than seasonal variability. The roughness measurements for the darkened pavement also exhibit more daily variability than seasonal variability but less overall variability than that of the typical pavement. Neither pavement temperature gradient nor moisture gradient appears to be correlated to roughness for either the typical pavement or the darkened pavement. Measurable curling and warping do not appear to be occurring at this site; the combination of joint spacing, slab thickness, steel reinforcement, and concrete strength at this site apparently minimized the occurrence of curling and warping.

Results related to laboratory testing include elastic modulus, compressive strength, rapid chloride permeability, Schmidt rebound hammer, and thermal conductivity of cylinders prepared from typical and darkened concrete. On average, the darkened concrete was stiffer than the typical concrete by 10.3 percent, stronger than the typical concrete by 17.2 percent, and less permeable than the typical concrete by 26.8 percent at 1 year. On average, the thermal conductivity of the darkened concrete was higher than that of the typical concrete by 7.7 percent, and the Schmidt rebound number of the darkened concrete was higher than that of the typical concrete by 13.9 percent.

5.3 Recommendations

The use of darkened concrete pavement to melt snow and ice more quickly than typical concrete pavement and to provide greater frost protection to subsurface layers and buried utilities during winter in cold regions is not recommended for sites similar to those investigated in this research. Numerical modeling of darkened concrete pavement to investigate the effects of greater intensity and/or duration of solar radiation is recommended for further study.

REFERENCES

Armaghani, J. M., T. J. Larsen, and L. L. Smith. (1987). "Temperature Response of Concrete Pavements." *Transportation Research Record*, 1121, 23-33.

Asaeda, T., V. T. Ca, and A. Wake. (1995). "Heat Storage of Pavement and Its Effect on the Lower Atmosphere." *Atmospheric Environment*, 30(3), 413-427.

Belshe, M., M. Mamlouk, K. Kaloush, and M. Rodezno. (2011). "Temperature Gradient and Curling Stresses in Concrete Pavement with and without Open-Graded Friction Course." *Journal of Transportation Engineering*, 137(10), 723-729.

Boriboonsomsin, K., and R. Reza. (2008). "Mix Design and Benefit Evaluation of High Solar Reflectance Concrete for Pavements." *Transportation Research Record: Journal of the Transportation Research Board*, 2011, 11-20.

Choubane, B., and M. Tia. (1995). "Analysis and Verification of Thermal-Gradient Effects on Concrete Pavement." *Journal of Transportation Engineering*, 121(1), 75-81.

Gajda, J. W., and M. G. Van Geem. (1997). "A Comparison of Six Environmental Impacts of Portland Cement Concrete and Asphalt Cement Concrete Pavement." *PCA R&D Serial 2068*, Portland Cement Association, Skokie, IL.

Guthrie, W. S., R. Bytheway, J. B. Dye, and D. L. Eggett. (2014). *Comparison of Wintertime Asphalt and Concrete Pavement Surface Temperatures on U.S. Route 40 near Heber, Utah*. Report No. UT-14.03, Utah Department of Transportation, Salt Lake City, UT.

Guthrie, W. S., and C. D. Thomas. (2014). *Deicer Usage on Concrete and Asphalt Pavements in Utah*. Report No. UT-14.02, Utah Department of Transportation, Salt Lake City.

Guthrie, W. S., T. Waters, and J. T. Knighton. (2016). "Thermal Behavior of Typical and Darkened Portland Cement Concrete Pavement: Applications to Winter Maintenance." Paper No. 16-6135. *Transportation Research Board 95th Annual Meeting*, Washington, DC.

Huang, Y. H. (2004). *Pavement Analysis and Design*, Second Edition. Pearson Prentice Hall, Upper Saddle River, New Jersey, 147-153.

Lange, D., C. Lee, and Y. Liu. (2006). "Prediction of Moisture Curling of Concrete Slabs for Airfield Applications." *Proceedings of the 2006 Airfield and Highway Pavements Specialty Conference*, Atlanta, GA.

Levinson, R., and H. Akbari. (2002). "Effects of Composition and Exposure on the Solar Reflectance of Portland Cement Concrete." *Cement and Concrete Research*, 32(11) 1679-1698.

Li, H., J. Harvey, and A. Kendall. (2013). "Field Measurement of Albedo for Different Land Cover Materials and Effects on Thermal Performance." *Building and Environment*, 59, 536-546.

Mailvaganam, N., J. Springfield, W. Repette, and D. Taylor. (2000). "Curling of Concrete Slabs on Grade." *Construction Technology Update No. 44*, National Research Council of Canada, Ottawa, Canada.

Nassiri, S., and J. Vandenbossche. (2011). "Establishing Built-in Temperature Gradient for Jointed Plain Concrete Pavements in Pennsylvania." *International Journal of Pavement Research & Technology*, 5(4), 245-256.

Paris, N., and M. Chusid. (1999). "Color in Concrete: Beauty and Durability." *Concrete International*, 21(1), 60-63.

Pera, J., R. Boumaza, and J. Ambroise. (1997). "Development of a Pozzolanic Pigment from Red Mud." *Cement and Concrete Research*, 27(10), 1513-1522.

Pomerantz, M., H. Akbari, A. Chen, H. Taha, and A. Rosenfeld. (1997). *Paving Materials for Heat Island Mitigation*. Lawrence Berkeley National Laboratory, Berkeley, CA.

Pomerantz, M., B. Pon, H. Akbari, and S. C. Chang. (2000a). *The Effect of Pavements' Temperatures on Air Temperatures in Large Cities*. Lawrence Berkeley National Laboratory, Berkeley, CA.

Pomerantz, M., H. Akbari., and J. Harvey. (2000b). *Cooler Reflective Pavements Give Benefits beyond Energy Savings: Durability and Illumination*. Lawrence Berkeley National Laboratory, Berkeley, CA.

Pomerantz, M., H. Akbari, S. C. Chang, R. Levinson, and B. Pon. (2003). *Examples of Cooler Reflective Streets for Urban Heat-Island Mitigation: Portland Cement Concrete and Chip Seals*. Lawrence Berkeley National Laboratory, Berkeley, CA.

Richard, C., Doré, G., Lemieux, C., Bilodeau, J-P, Haure-Touzé, J. (2015). "Albedo of Pavement Surfacing Materials: In Situ Measurements." *Proceedings of the American Society of Civil Engineers Sixteenth International Conference on Cold Regions Engineering*, Salt Lake City, UT.

Richart, F. E., J. R. Hall, and R. D. Woods. (1970). *Vibrations of Soils and Foundations*. Prentice-Hall, Englewood Cliffs, NJ.

Siddique, Z. Q., M. Hossain, J. Devore, and W. H. Parcells. (2003). "Effect of Curling on As-Constructed and Early Life Smoothness of PCC Pavements." *Proceedings of the 2003 Mid-Continent Transportation Research Symposium*, Ames, IA.

Siddique, Z. Q., M. Hossain, and J. Devore. (2004). *Investigation of the Effect of Curling on As-Constructed Smoothness and Ride Quality of KDOT Portland Cement Concrete (PCC) Pavements*. Report No. K-TRAN: KSU-01-7, Kansas Department of Transportation, Topeka, KS.

Siddique, Z. Q., and M. Hossain. (2005). "Finite Element Analysis of PCCP Curling and Roughness." *Eighth International Conference on Concrete Pavements*, Colorado Springs, CO.

Sumsion, E. S., and W. S. Guthrie. (2013). *Physical and Chemical Effects of Deicers on Concrete Pavement: Literature Review*. Report No. UT-13.09. Utah Department of Transportation, Salt Lake City, UT.

Synnefa, A., T. Karlessi, N. Gaitani, and M. Santamouris. (2009). "Measurement of Optical Properties and Thermal Performance of Coloured Thin Layer Asphalt Samples and Evaluation of Their Impact on the Urban Environment." *The Second International Conference on Countermeasures to Urban Heat Islands*, Berkeley, CA.

Ting, M., J. Koomey, and M. Pomerantz. (2001). *Preliminary Evaluation of the Lifecycle Costs and Market Barriers of Reflective Pavements*. Lawrence Berkeley National Laboratory, Berkeley, CA.

Utah Department of Transportation. *UDOT Maintenance Facts*. www.udot.utah.gov/main/uconowner.gf?n=2253002476382780. Accessed June 10, 2011.

Wang, S. (2015) *Pavement Albedo Assessment: Methods, Aspects, and Implication*. Thesis, Iowa State University, Ames, IA.

Wong, C. W., N. H. Wong, T. P. Ping, and A. Z. W. Aloysius. (2009). A Study on the Effectiveness of Heat Mitigating Pavement Coatings in Singapore. *The Second International Conference on Countermeasures to Urban Heat Islands*, Berkeley, CA.

Yavuzturk, C., K. Ksaibati, and A. D. Chiasson. (2005). "Assessment of Temperature Fluctuations in Asphalt Pavements Due to Thermal Environmental Conditions Using a Two-Dimensional, Transient Finite-Difference Approach." *Journal of Materials in Civil Engineering*, 17(4), 465-475.

Youssef, E. A. M., N. M. Ahmed, and M. A. Abd El-Ghaffar. (1998). "Characterization and Evaluation of Silica Fume as an Extender Pigment for Surface Coating Applications." *Pigment & Resin Technology*, 27(2), 88-98.

APPENDIX A: FIELD DATA

This appendix includes tables and figures providing relevant supporting data for the field testing performed in this research. The presence of a hyphen in a table indicates that the given data were not measured. Tables A-1 and A-2 present average transverse and longitudinal slopes, respectively, for each section. Table A-3 presents pavement albedo values for each section.

Table A-4 presents average surface temperatures for each testing time, and Figures A-1 through A-18 show typical infrared images from each site at each testing time.

Table A-1: Transverse Slopes

Survey Location			Average Transverse Slope (%)
Site 1	Typical	East	-0.5
		West	-2.3
	Darkened	East	0.3
		West	-2.2
Site 2	Typical	East	-2.3
		West	0.1
	Darkened	East	-1.8
		West	1.1
Site 3	Typical	East	-2.0
		West	-1.8
	Darkened	East	1.4
		West	-2.3

Table A-2: Longitudinal Slopes

Survey Location			Average Longitudinal Slope (%)
Site 1	Typical	North	-2.6
		South	-2.9
	Darkened	North	-3.6
		South	-2.6
Site 2	Typical	North	-1.3
		South	-0.5
	Darkened	North	-0.5
		South	-0.8
Site 3	Typical	North	-0.2
		South	-0.1
	Darkened	North	-0.2
		South	-0.2

Table A-3: Pavement Albedo Values

Pavement Condition	Pavement Albedo		
	Typical	Darkened	Asphalt
Dry	0.313	0.211	0.157
Wet	0.294	0.195	0.154

Table A-4: Average Pavement Surface Temperatures

Date	Time	Site	Concrete Type	Average Surface Temperature (°F)
June 7, 2014	11:59 AM	1	Typical	90.9
			Darkened	102.6
		2	Typical	104.5
			Darkened	97.2
	3:04 PM	1	Typical	103.9
			Darkened	116.7
		2	Typical	115.5
			Darkened	110.4
	6:36 PM	1	Typical	89.6
			Darkened	99.3
		2	Typical	97.2
			Darkened	93.0
	10:11 PM	1	Typical	72.2
			Darkened	78.3
		2	Typical	78.8
			Darkened	76.1
June 8, 2014	7:50 AM	1	Typical	59.5
			Darkened	63.8
		2	Typical	68.0
			Darkened	65.8
September 6, 2014	1:09 PM	1	Typical	88.6
			Darkened	97.8
		2	Typical	99.5
			Darkened	93.0
	3:52 PM	1	Typical	99.3
			Darkened	107.9
		2	Typical	107.4
			Darkened	101.8
	5:22 PM	1	Typical	94.5
			Darkened	104.2
		2	Typical	101.4
			Darkened	96.4
	9:17 PM	1	Typical	72.0
			Darkened	78.1
		2	Typical	76.8
			Darkened	73.6
September 7, 2014	8:27 AM	1	Typical	59.1
			Darkened	62.2
		2	Typical	65.6
			Darkened	63.1

Table A-4: Average Pavement Surface Temperatures, Continued

| Date	Time	Site	Concrete Type	Average Surface Temperature (°F)
June 7, 2014	11:59 AM	1	Typical	90.9
			Darkened	102.6
		2	Typical	104.5
			Darkened	97.2
	3:04 PM	1	Typical	103.9
			Darkened	116.7
		2	Typical	115.5
			Darkened	110.4
	6:36 PM	1	Typical	89.6
			Darkened	99.3
		2	Typical	97.2
			Darkened	93.0
	10:11 PM	1	Typical	72.2
			Darkened	78.3
		2	Typical	78.8
			Darkened	76.1
June 8, 2014	7:50 AM	1	Typical	59.5
			Darkened	63.8
		2	Typical	68.0
			Darkened	65.8
September 6, 2014	1:09 PM	1	Typical	88.6
			Darkened	97.8
		2	Typical	99.5
			Darkened	93.0
	3:52 PM	1	Typical	99.3
			Darkened	107.9
		2	Typical	107.4
			Darkened	101.8
	5:22 PM	1	Typical	94.5
			Darkened	104.2
		2	Typical	101.4
			Darkened	96.4
	9:17 PM	1	Typical	72.0
			Darkened	78.1
		2	Typical	76.8
			Darkened	73.6
September 7, 2014	8:27 AM	1	Typical	59.1
			Darkened	62.2
		2	Typical	65.6
			Darkened	63.1

66

(a)

(b)

Figure A-1: Typical infrared images from November 16, 2013 at 5:15 PM for (a) site 1 and (b) sites 2 and 3.
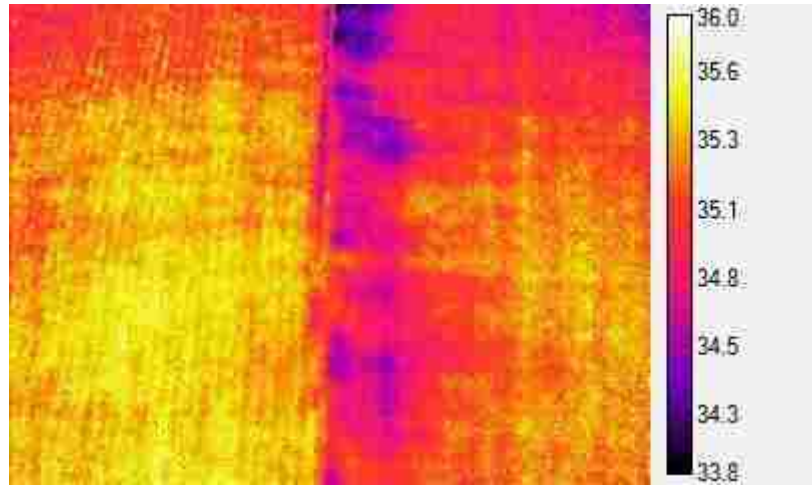
(a)
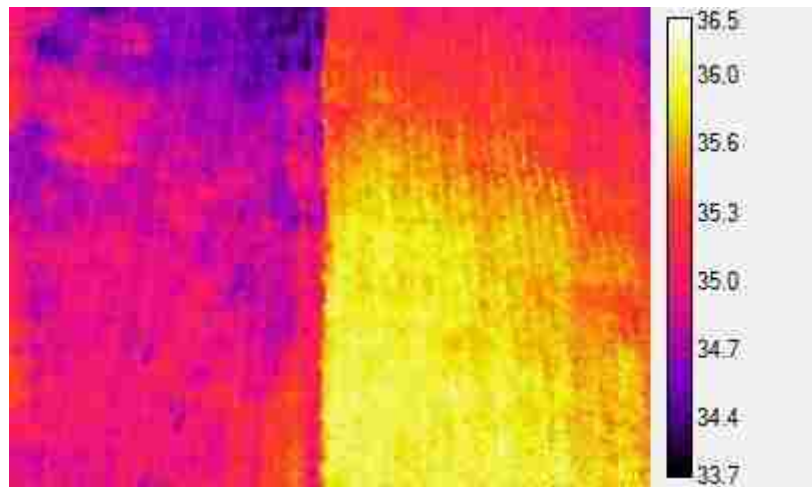
(b)

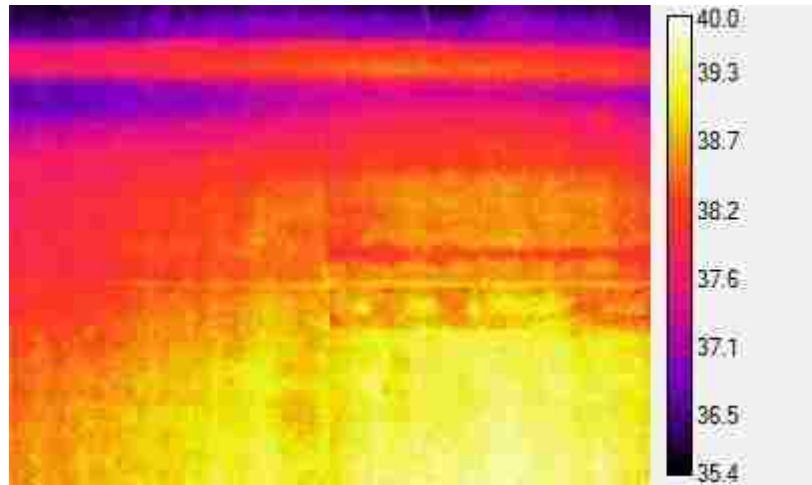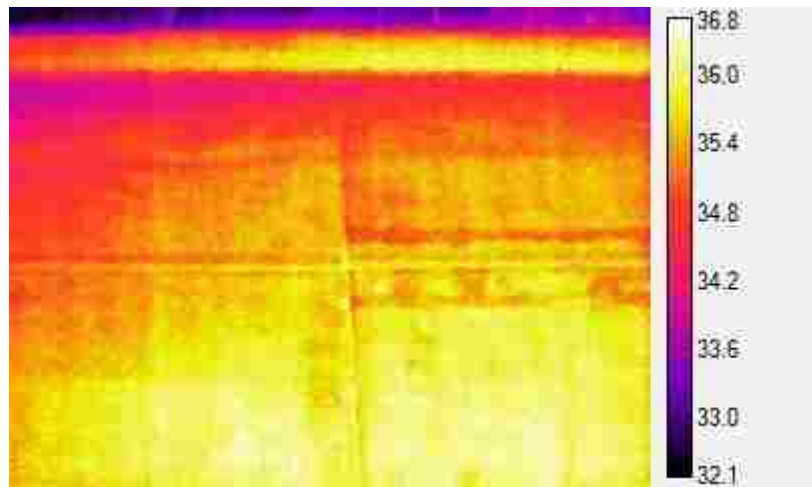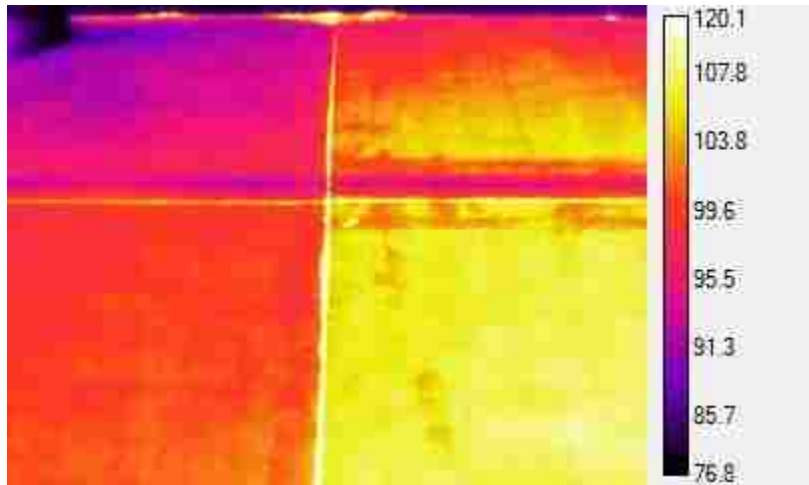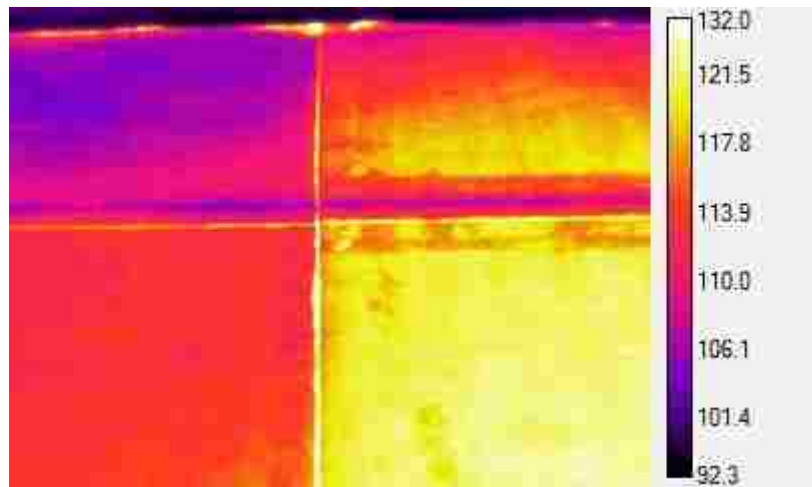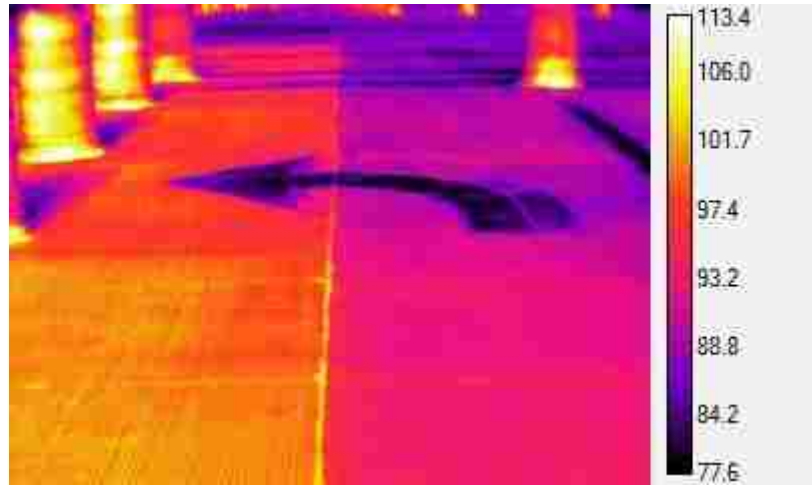**Figure A-2: Typical infrared images from November 16, 2013 at 9:31 PM for (a) site 1 and (b) sites 2 and 3.**
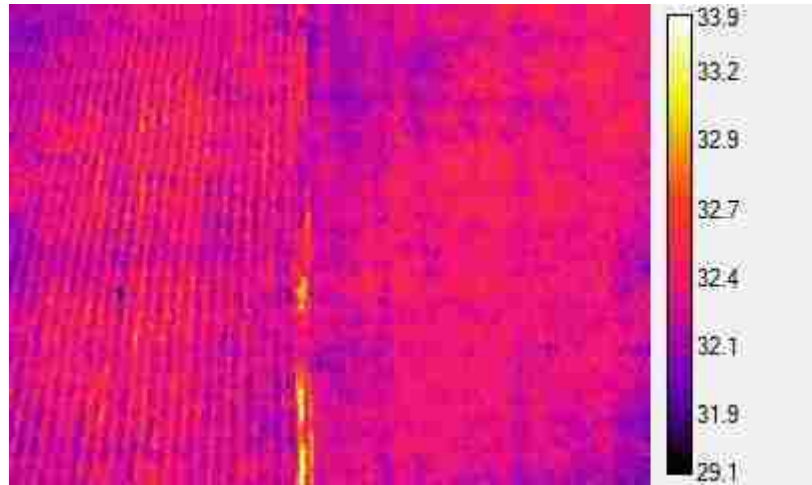
(a)
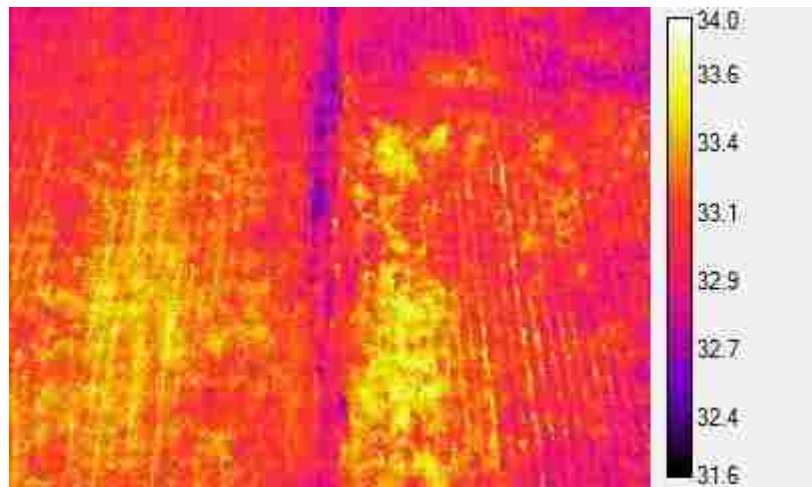
(b)

Figure A-3: Typical infrared images from November 17, 2013 at 6:53 AM for (a) site 1 and (b) sites 2 and 3.
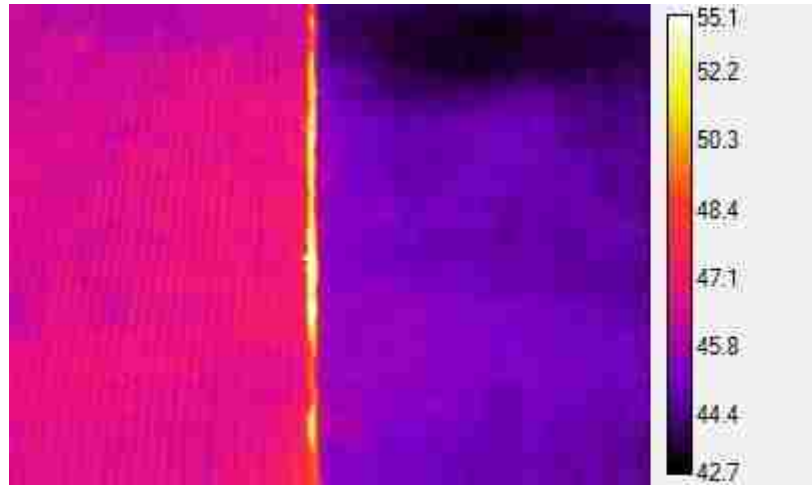
(a)
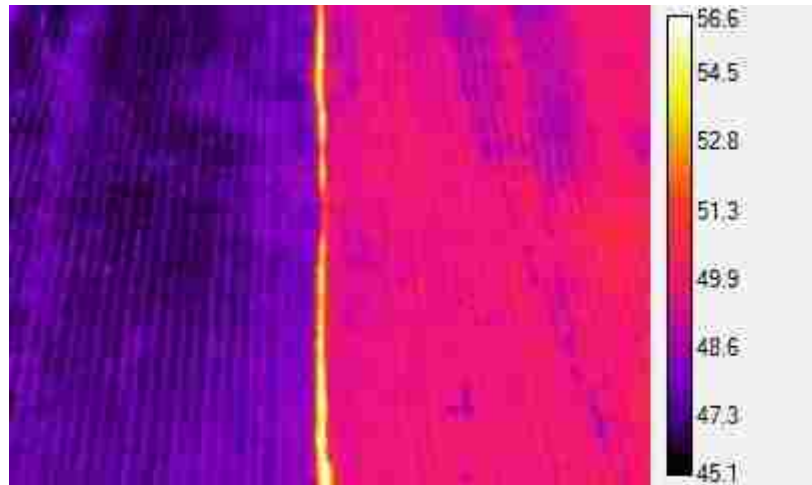
(b)

Figure A-4: Typical infrared images from November 17, 2013 at 12:02 PM for (a) site 1 and (b) sites 2 and 3.
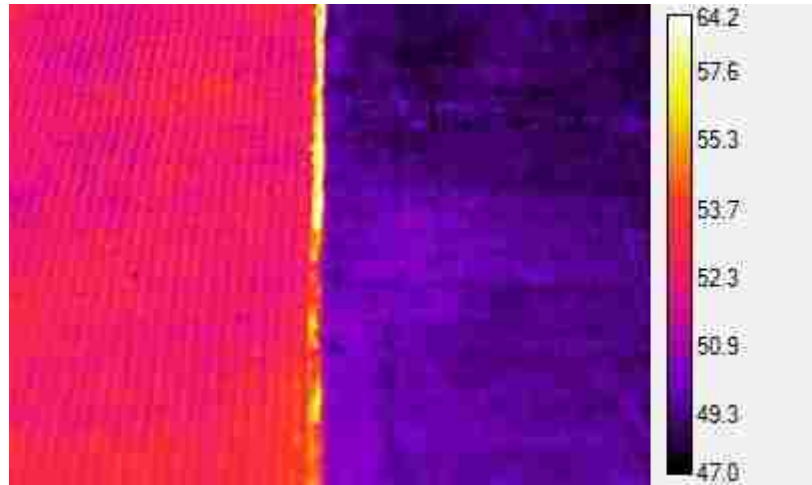
(a)
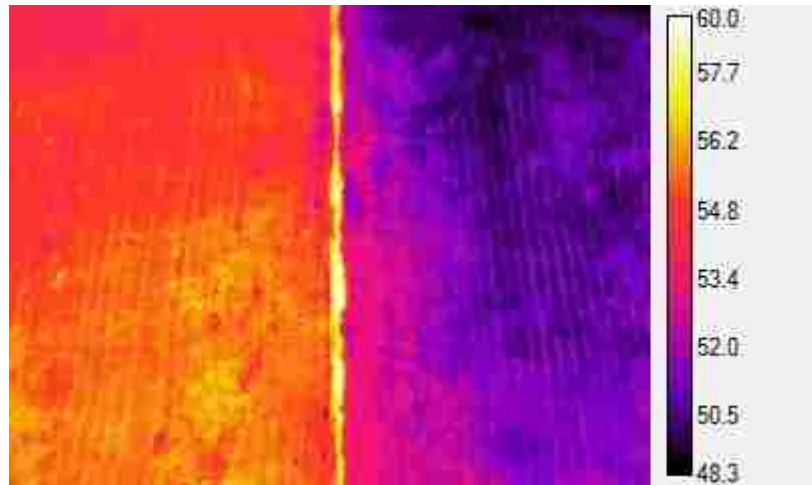
(b)

Figure A-5: Typical infrared images from November 17, 2013 at 2:48 PM for (a) site 1 and (b) sites 2 and 3.
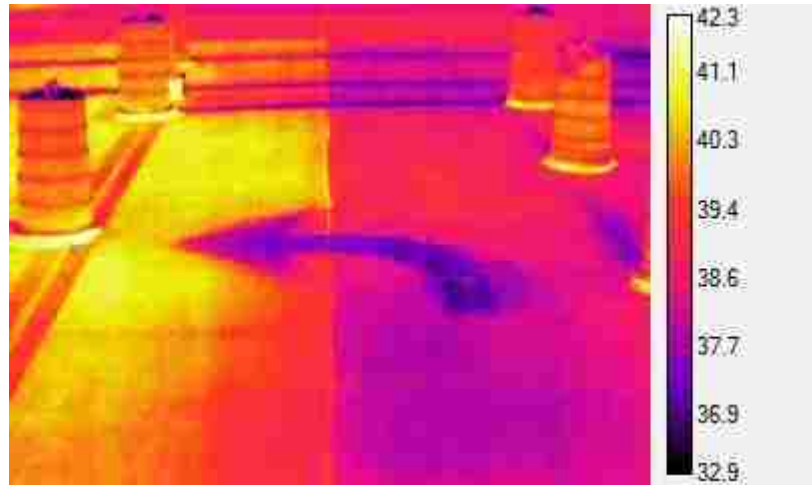
(a)
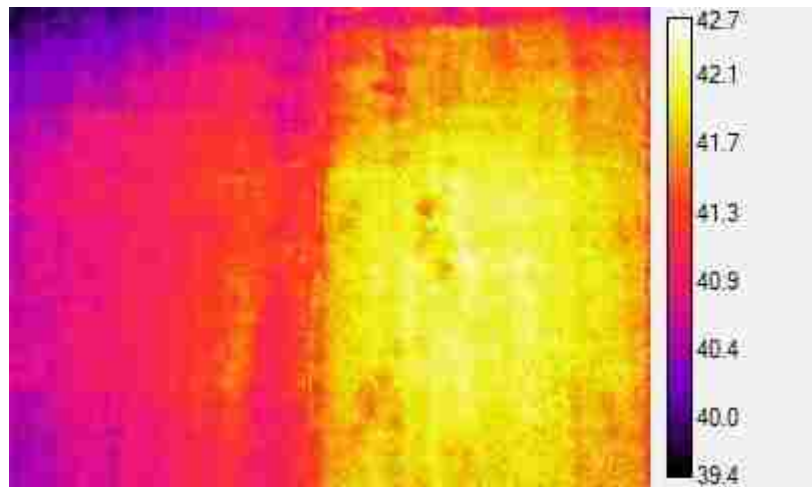
(b)

Figure A-6: Typical infrared images from February 15, 2014 at 5:39 PM for (a) site 1 and (b) sites 2 and 3.
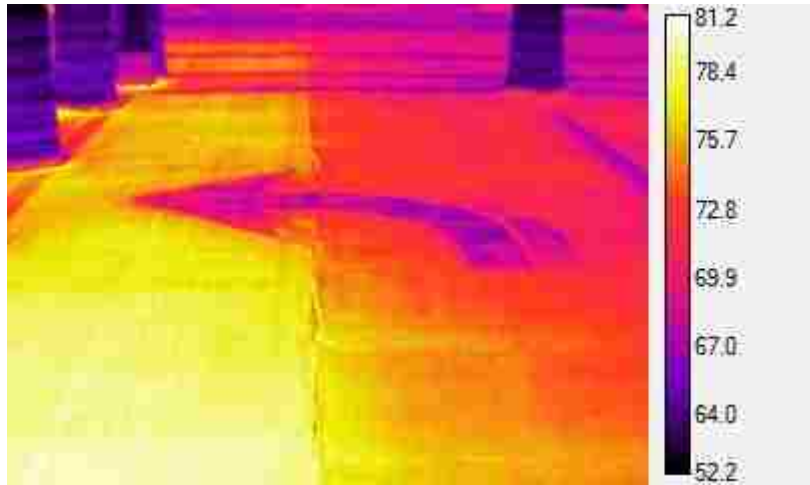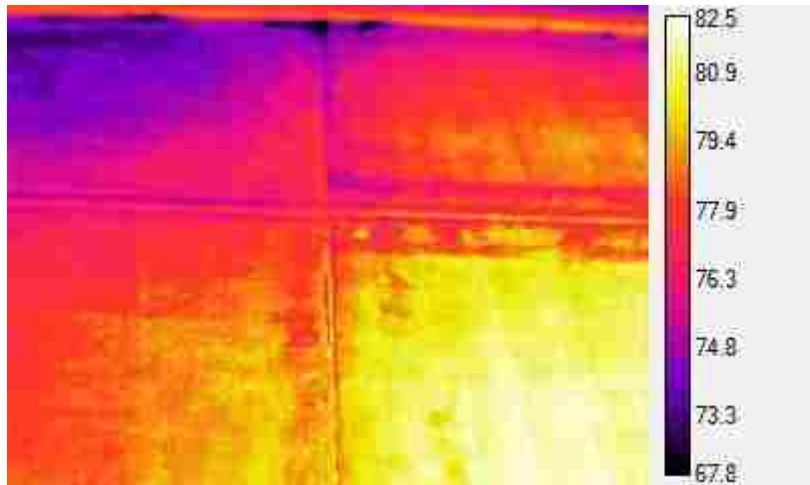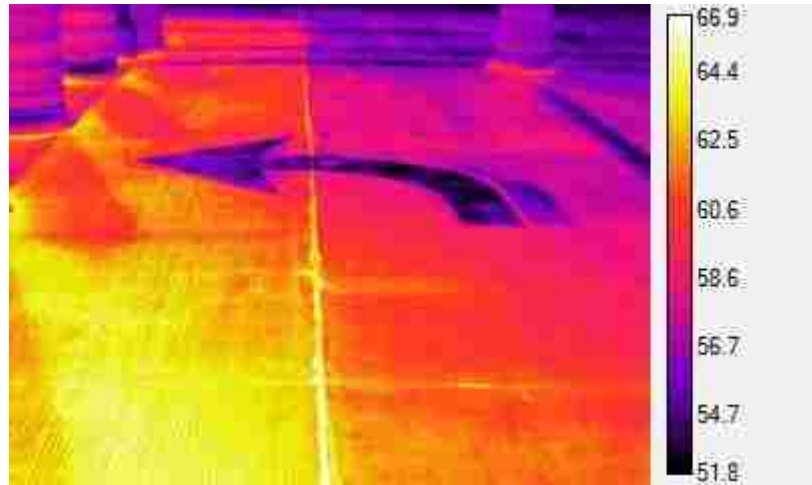
Figure A-7: Typical infrared images from February 15, 2014 at 9:08 PM for (a) site 1 and (b) sites 2 and 3.

(a)

(b)

Figure A-8: Typical infrared images from February 16, 2014 at 7:05 PM for (a) site 1 and (b) sites 2 and 3.

(a)

(b)

Figure A-9: Typical infrared images from June 7, 2014 at 11:59 AM for (a) site 1 and (b) sites 2 and 3.
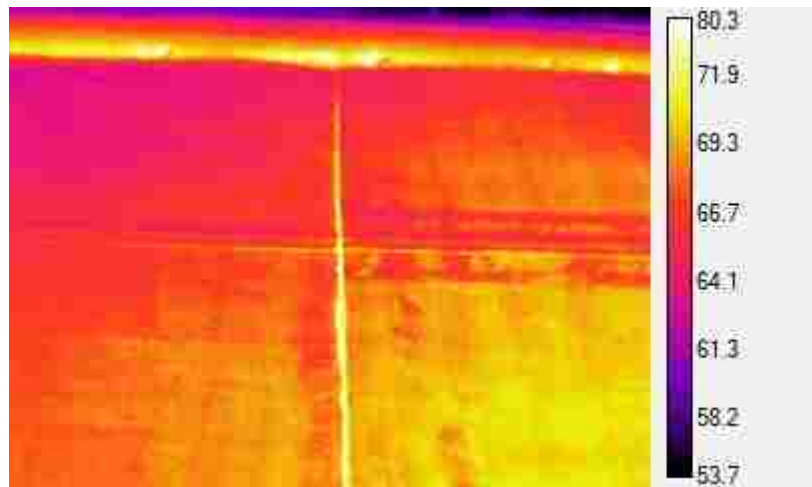
(a)

(b)

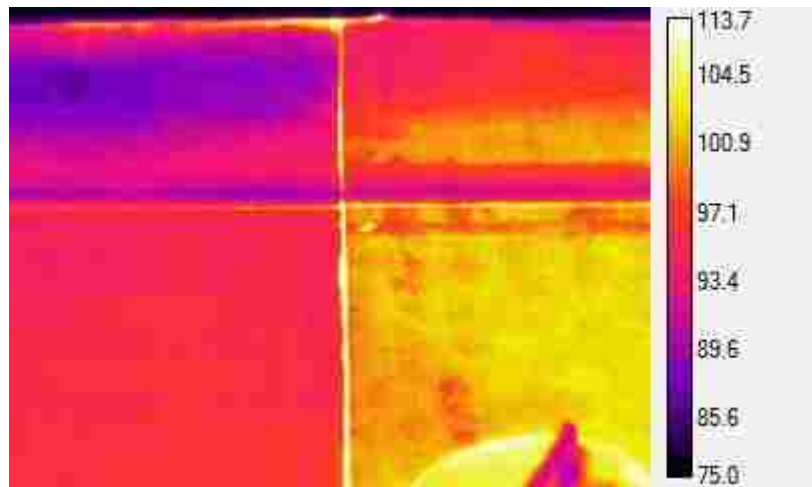**Figure A-10: Typical infrared images from June 7, 2014 at 3:04 PM for (a) site 1 and (b) sites 2 and 3.**

(a)
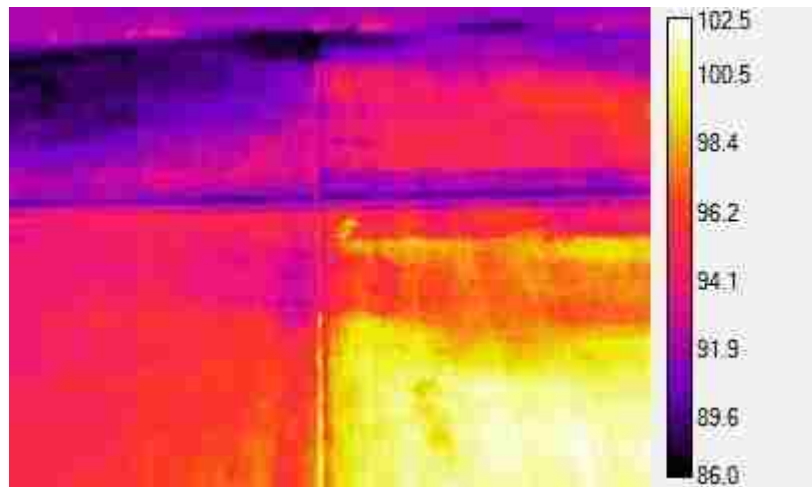
(b)

Figure A-11: Typical infrared images from June 7, 2014 at 6:36 PM for (a) site 1 and (b) sites 2 and 3.

(a)

(b)

Figure A-12: Typical infrared images from June 7, 2014 at 10:11 PM for (a) site 1 and (b) sites 2 and 3.

(a)

(b)

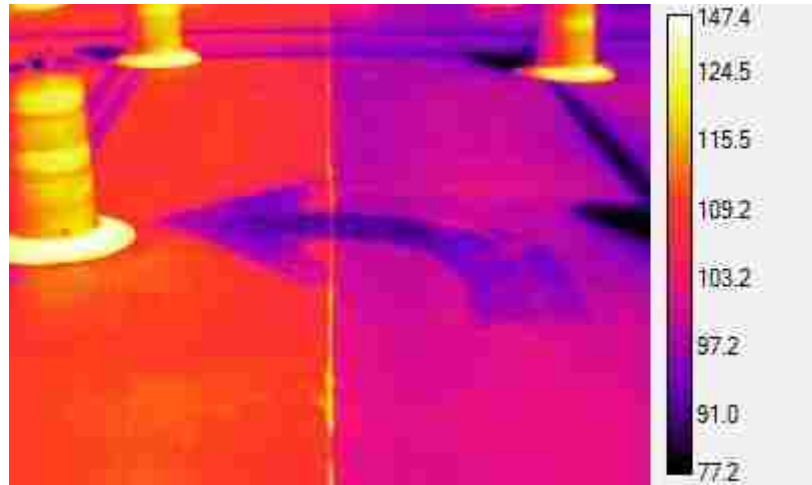**Figure A-13: Typical infrared images from June 8, 2014 at 7:50 AM for (a) site 1 and (b) sites 2 and 3.**

(a)

(b)

Figure A-14: Typical infrared images from September 6, 2014 at 1:09 PM for (a) site 1 and (b) sites 2 and 3.
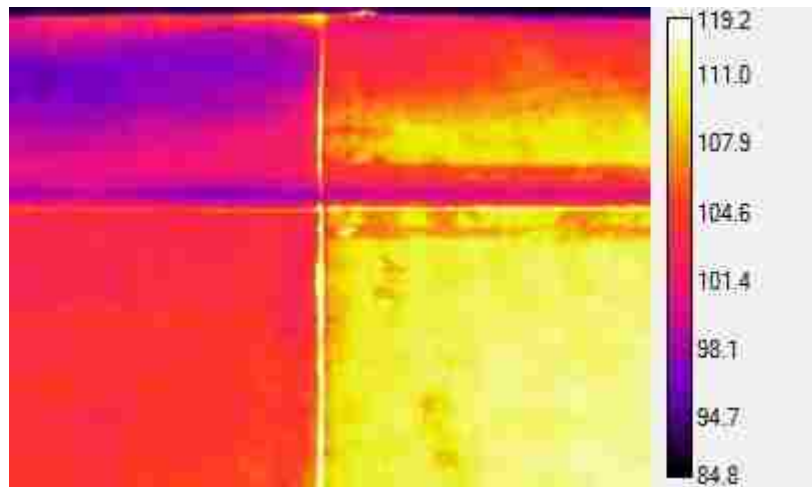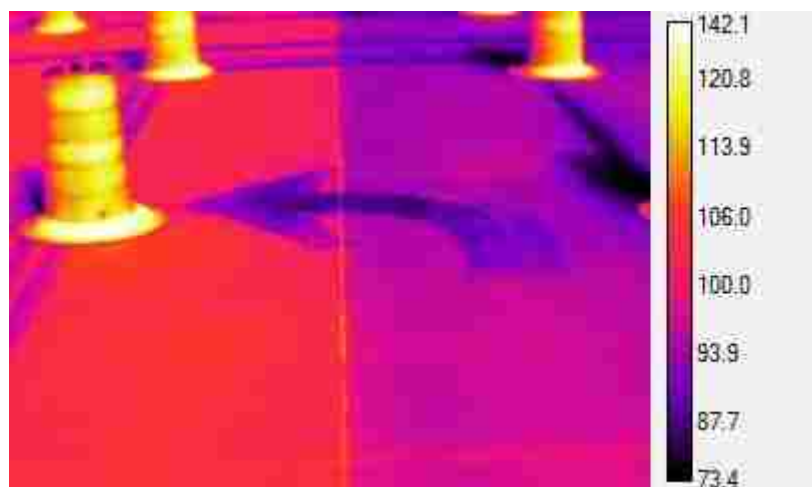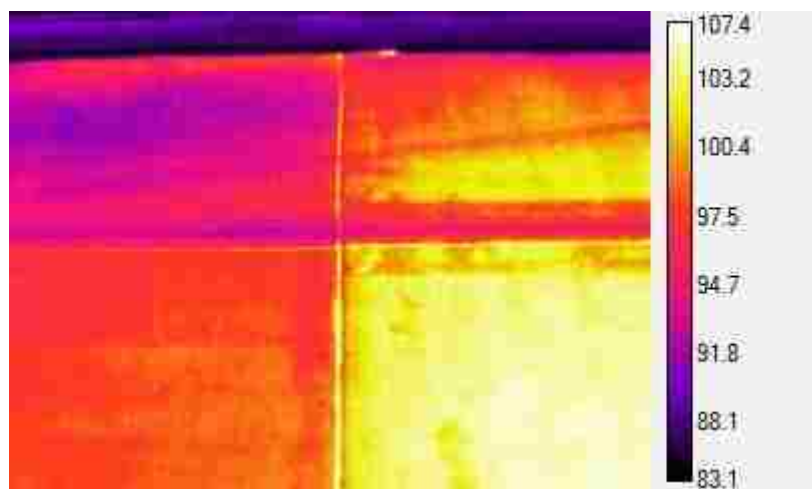
(a)

(b)

Figure A-15: Typical infrared images from September 6, 2014 at 3:52 PM for (a) site 1 and (b) sites 2 and 3.
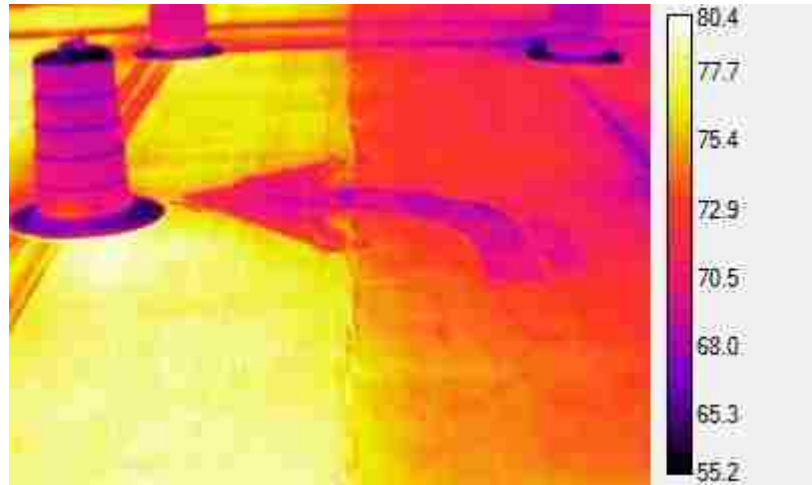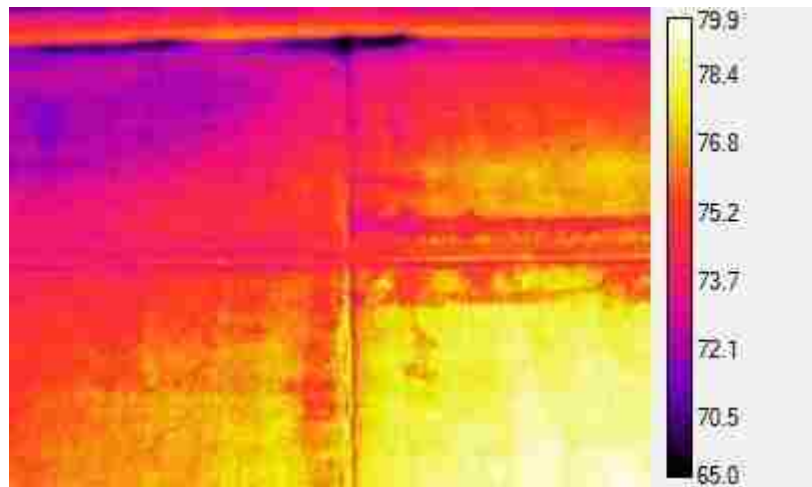
(a)

(b)

Figure A-16: Typical infrared images from September 6, 2014 at 5:22 PM for (a) site 1 and (b) sites 2 and 3.
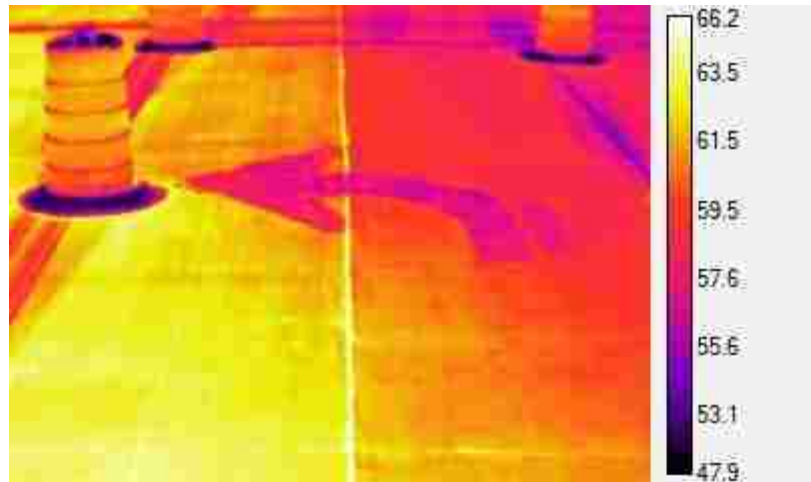
(a)

(b)

Figure A-17: Typical infrared images from September 6, 2014 at 9:17 PM for (a) site 1 and (b) sites 2 and 3.

(a)
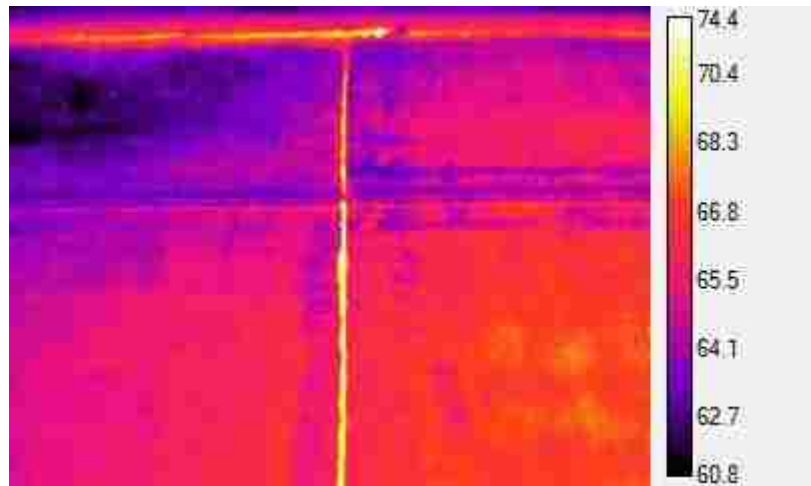
(b)

Figure A-18: Typical infrared images from September 7, 2014 at 8:27 AM for (a) site 1 and (b) sites 2 and 3.

Figures A-19 through A-23 document ambient conditions measured using the environmental sensors. During the two-year monitoring period, the air temperature at the research site ranged from approximately 0°F during the winter to 100°F during the summer, as shown in Figure A-19. On a given day, the difference between the maximum and minimum air temperature ranged from about 25°F to 50°F. Figure A-20 shows that, on average, relative

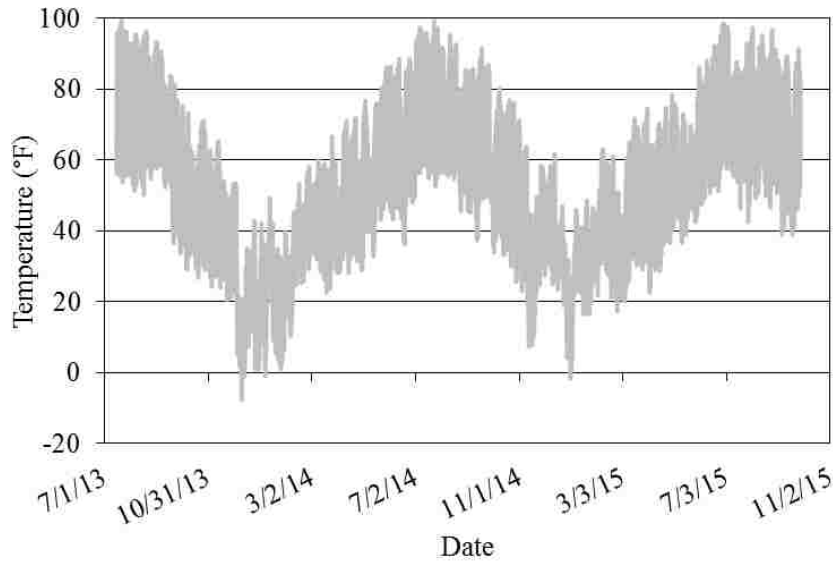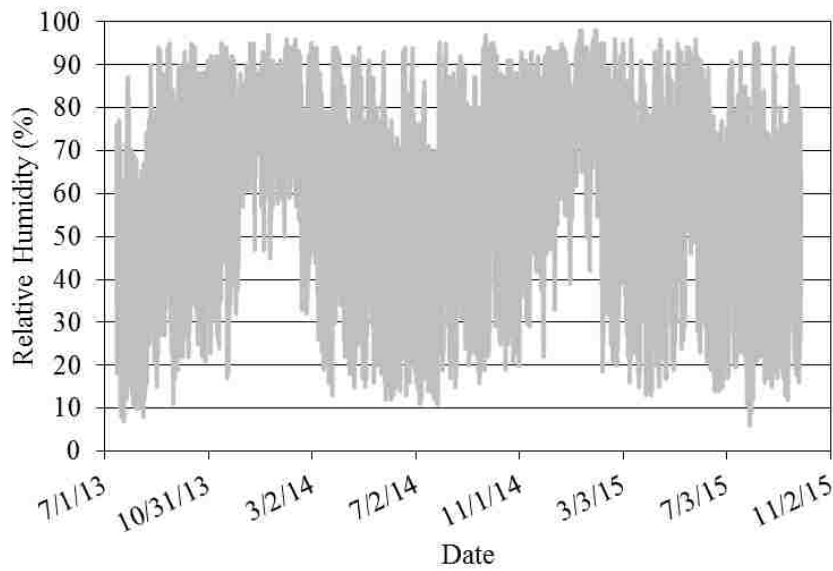**Figure A-19: Air temperature from environmental sensor.**

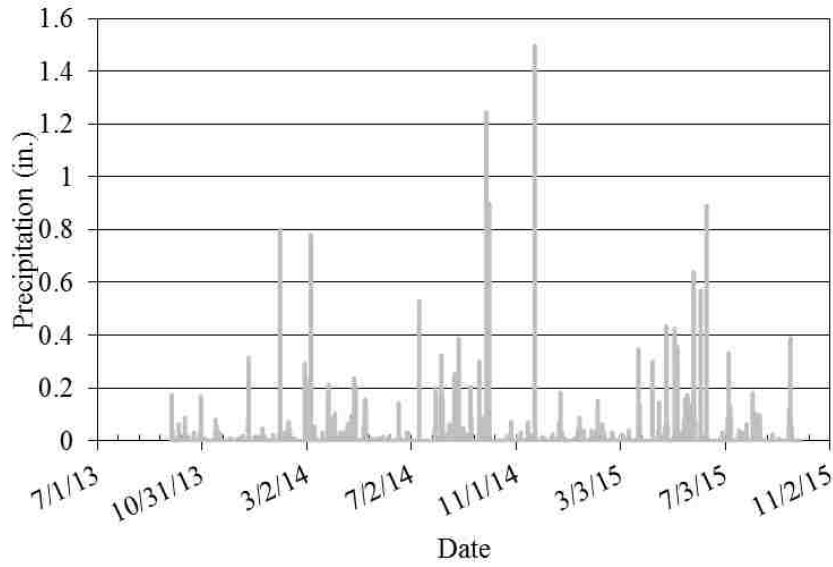**Figure A-20: Relative humidity from environmental sensor.**

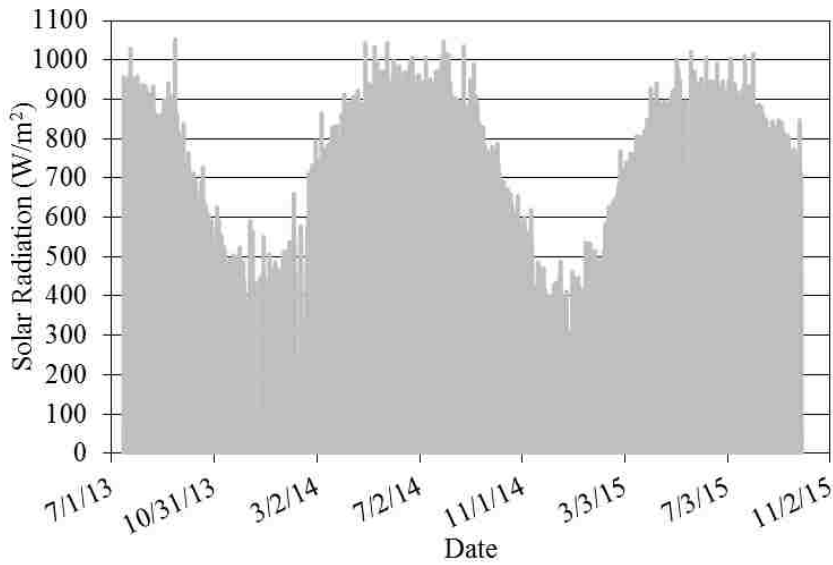**Figure A-21: Precipitation from environmental sensor.**

Figure A-22: Solar radiation measurements from Campbell Scientific, Inc.
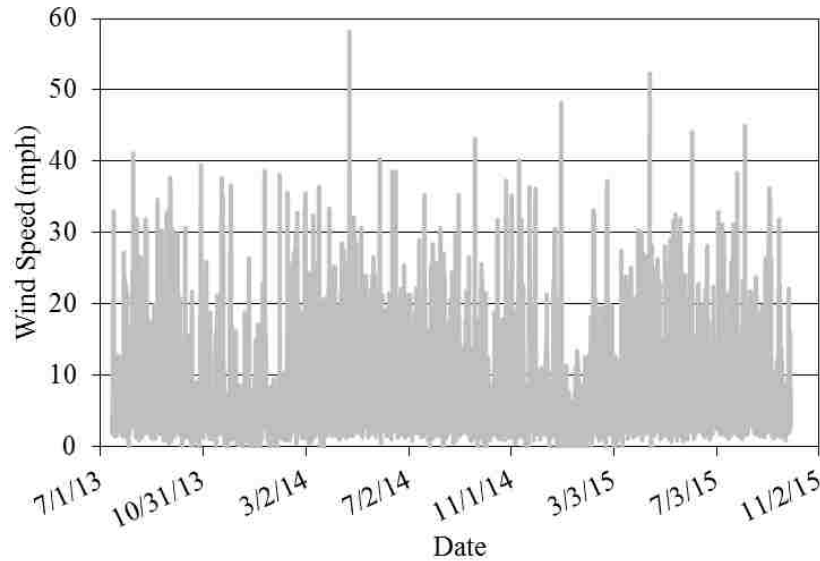
Figure A-23: Wind speed measurements from Campbell Scientific, Inc.

humidity is higher during the winter and lower during the summer, and Figure A-21 shows that precipitation varies through the year with greater amounts measured during the spring and fall.

Figure A-22 shows solar radiation data collected by Campbell Scientific, Inc. at their headquarters located near the intersection studied in this research. The average magnitude of solar radiation during the winter is about half that of the solar radiation during the summer.

Figure A-23 shows wind speed data, also collected by Campbell Scientific, Inc. at their headquarters. Wind speed in this region varies throughout the year and is typically lower during the winter months.

Figures A-24 and A-25 show upper and lower pavement temperature, respectively, as measured by the embedded sensors. When considered over the entire monitoring period, the upper pavement temperature of the darkened concrete pavement was generally a few degrees higher than that of the typical concrete pavement, as shown in Figure A-24. Likewise, Figure A-25 shows that the lower pavement temperature of the darkened concrete pavement was also

generally a few degrees higher than that of the typical concrete pavement. As previously explained, the lower sensor in the typical concrete at site 3 apparently malfunctioned beginning in May 2014, and temperature, moisture, and electrical conductivity data from that sensor are consequently excluded beyond that date.
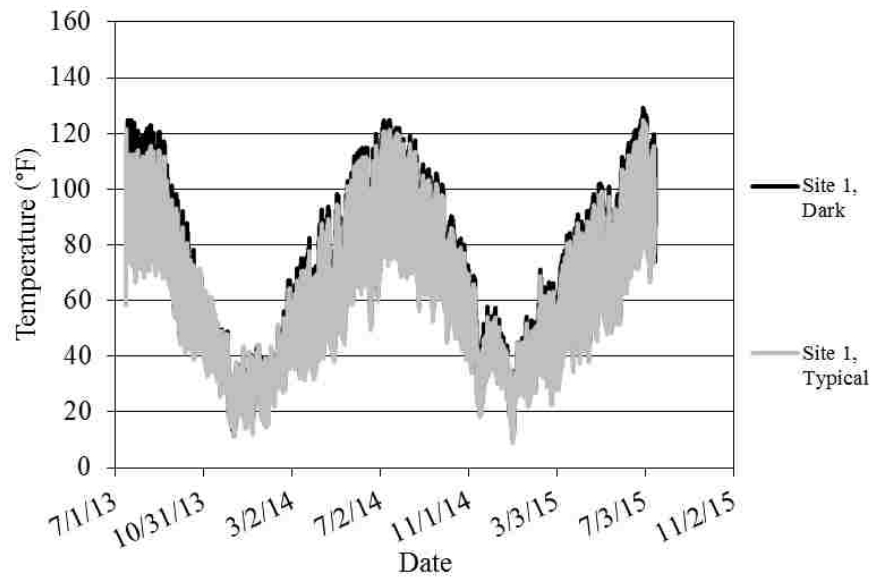
(a)
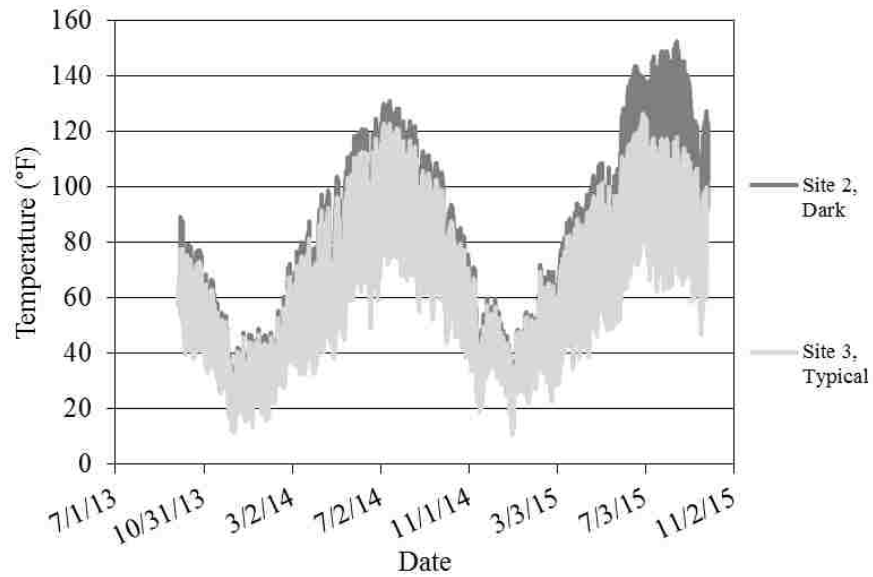
(b)

Figure A-24: Upper pavement temperature for (a) site 1 and (b) sites 2 and 3.
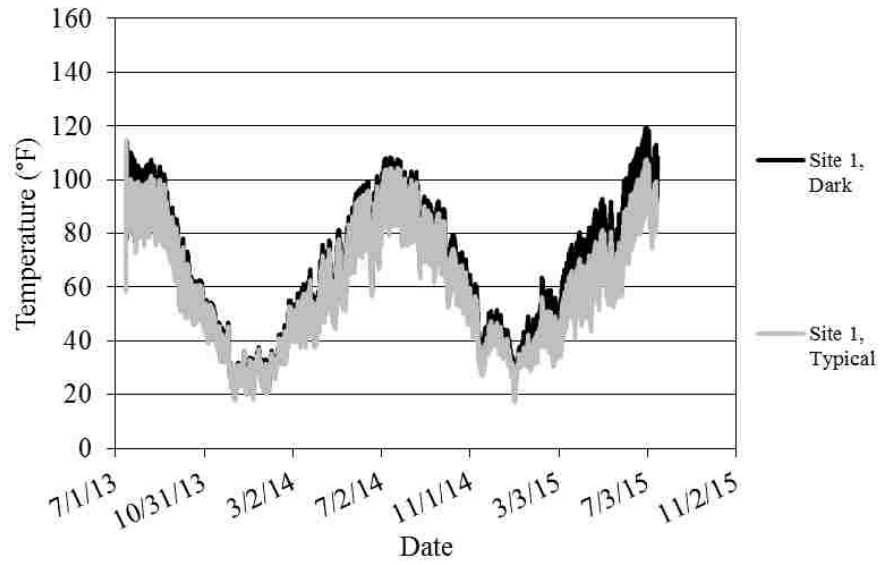
(a)
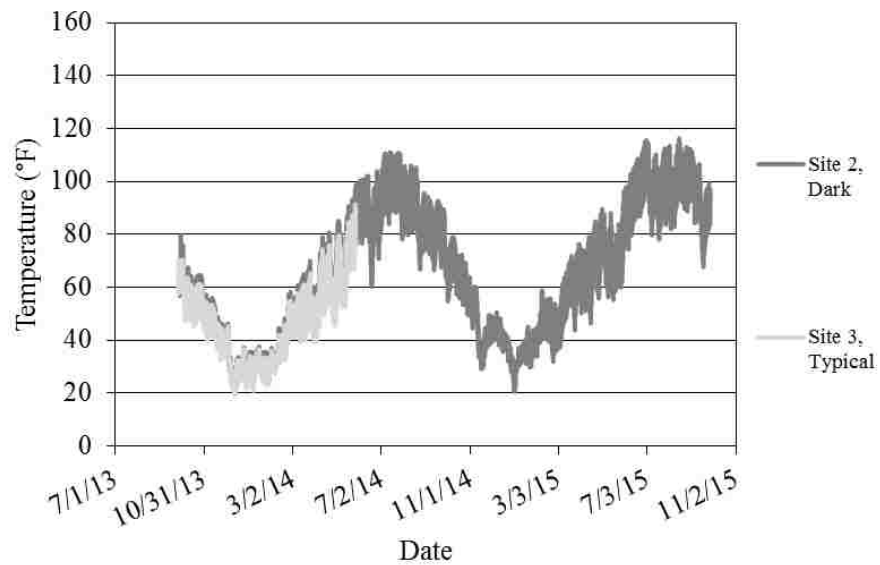
(b)

Figure A-25: Lower pavement temperature for (a) site 1 and (b) sites 2 and 3.

Figures A-26 and A-27 show the upper and lower pavement moisture, respectively, as measured by the embedded sensors. The upper pavement moisture content was at its peak at the time of concrete placement and then stabilized at values generally ranging between 15 and 25 percent, as shown in Figure A-26. The darkened concrete pavement had a consistently higher

moisture content than the typical concrete pavement. Likewise, Figure A-27 shows that the

lower pavement moisture content was also at its peak at the time of concrete placement but

stabilized to lower values generally ranging between 10 and 20 percent.

(a)

(b)
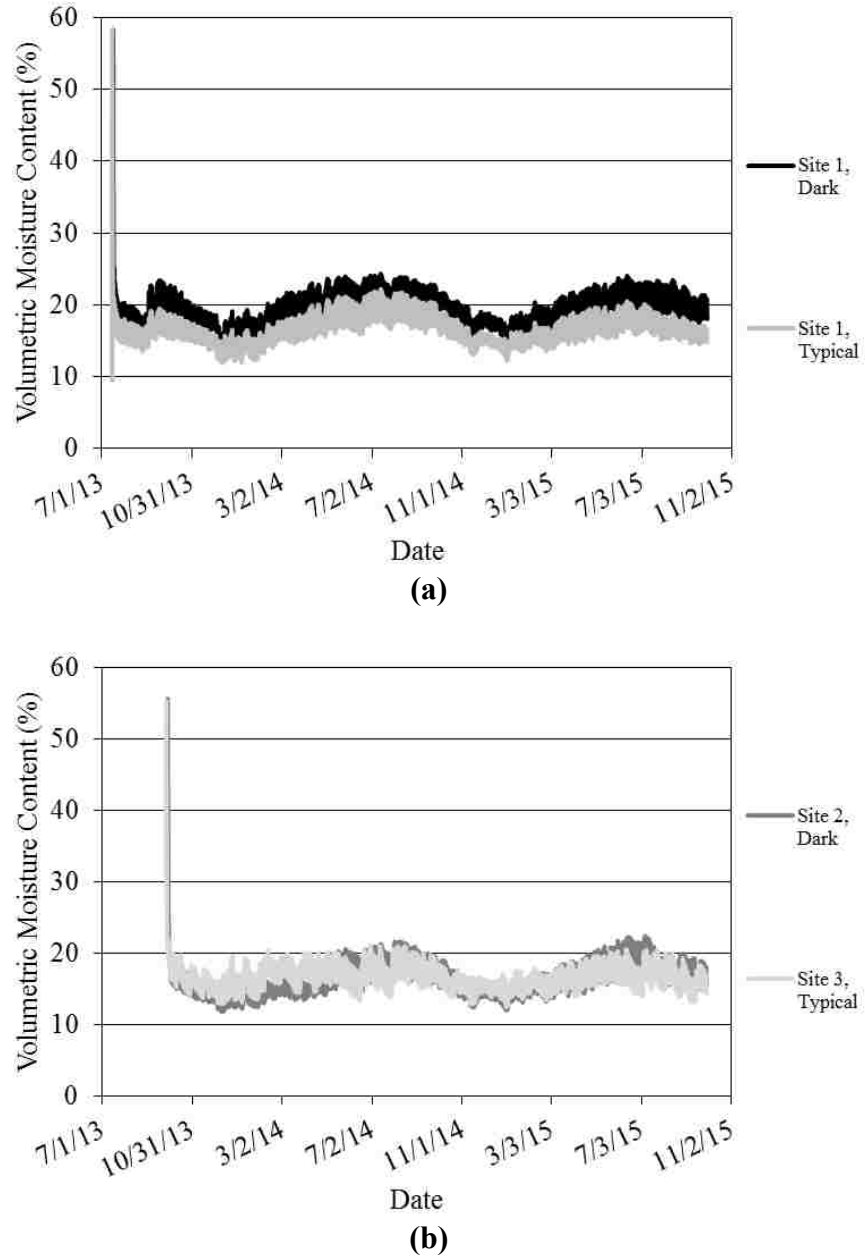
Figure A-26: Upper pavement moisture for (a) site 1 and (b) sites 2 and 3.
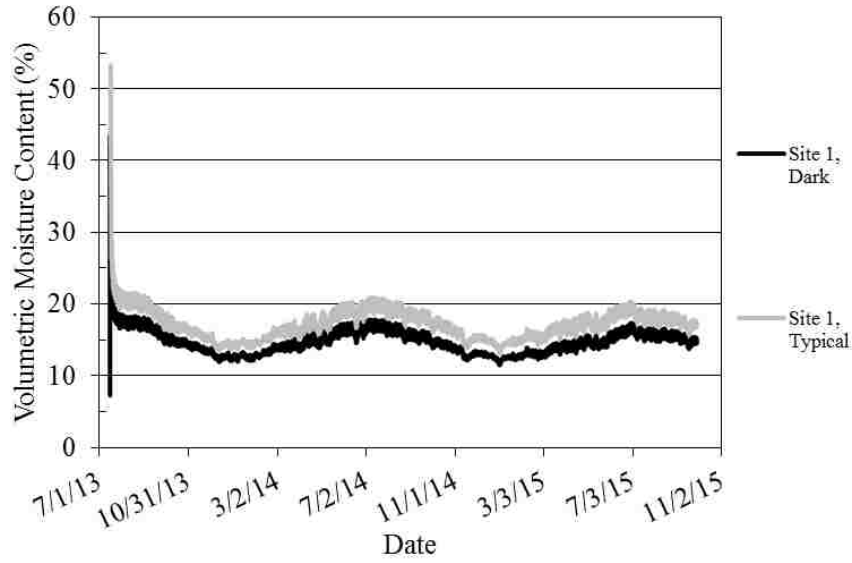
(a)
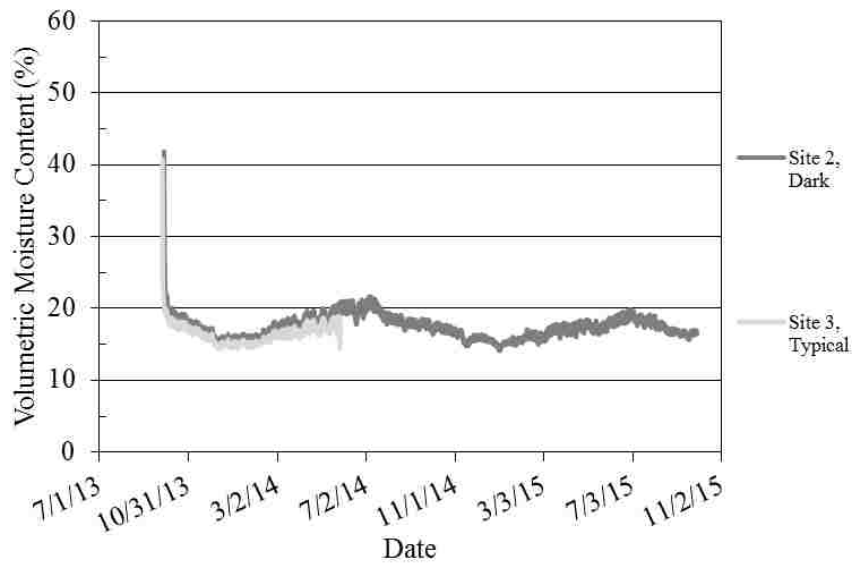
(b)

Figure A-27: Lower pavement moisture for (a) site 1 and (b) sites 2 and 3.

Figures A-28 and A-29 show the upper and lower pavement electrical conductivity, respectively, as measured by the embedded sensors. On average, there is no measurable difference in upper or lower electrical conductivity between the two types of concrete.
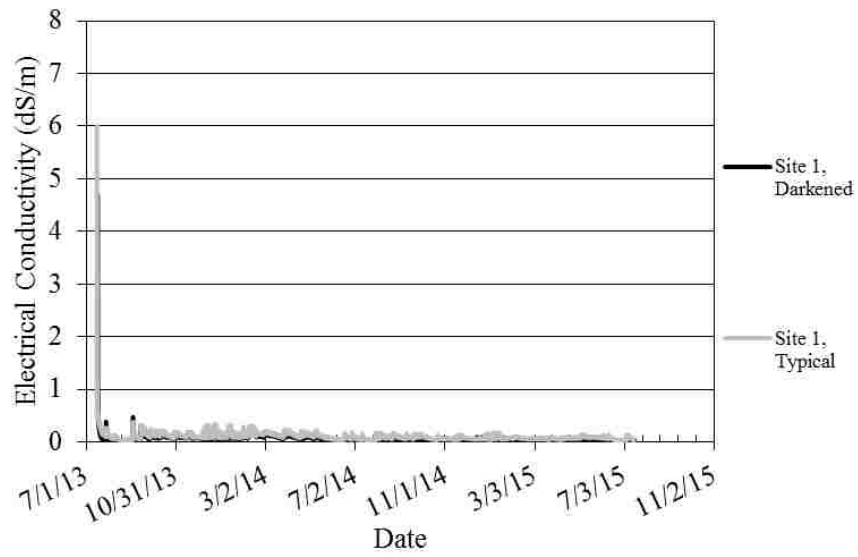
(a)
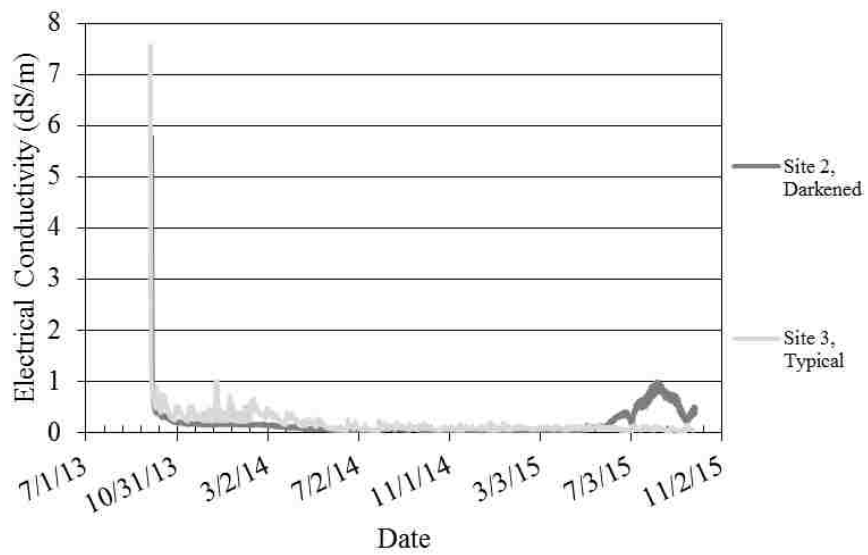
(b)

Figure A-28: Upper pavement electrical conductivity for (a) site 1 and (b) sites 2 and 3.

92
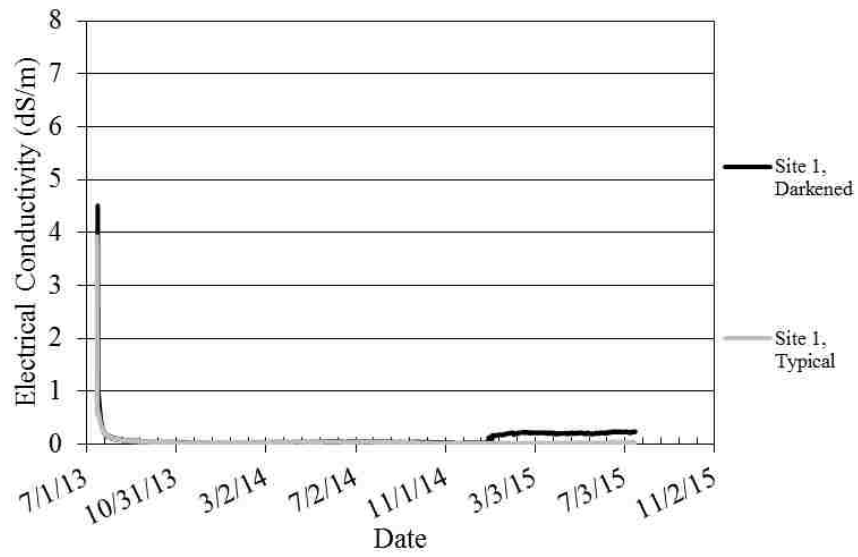
(a)
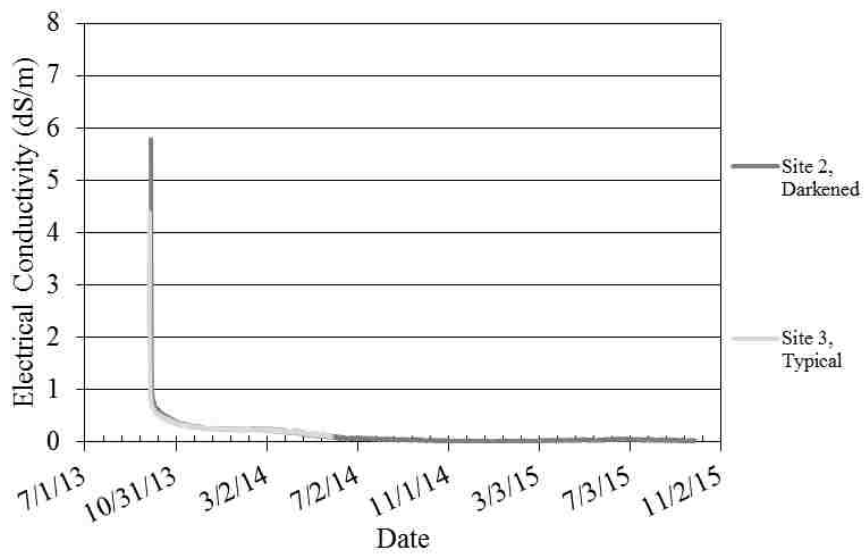
(b)

Figure A-29: Lower pavement electrical conductivity for (a) site 1 and (b) sites 2 and 3

APPENDIX B: LABORATORY DATA

This appendix includes tables and figures providing relevant supporting data for the laboratory testing performed in this research. The presence of a hyphen in a table indicates that the given data were not measured. Table B-1 gives cylinder properties and elastic modulus values of all cylinders tested. A noticeable difference between the elastic modulus values of the typical and darkened concrete was not observed.

Table B-2 gives loads and compressive strengths of all cylinders tested. The comparatively low strength of the typical concrete at site 3 is likely the result of heavy rain during the concrete placement. At the time of the rainstorm, the concrete cylinders were still being cast, and the concrete pavement was still being finished. On average, the darkened concrete was slightly stronger than the typical concrete.

Table B-3 gives rapid chloride permeability values and classifications for all cylinders tested. Again, the comparatively high permeability of the typical concrete at site 3 is likely the result of heavy rain during the concrete placement. On average, the darkened concrete was slightly less permeable than the typical concrete.

Table B-4 gives thermal conductivity values and temperatures for all cylinders tested. In most cases, the darkened concrete had a higher thermal conductivity than the typical concrete.

Table B-5 gives Schmidt rebound hammer values for all cylinders tested. On average, the darkened concrete had higher Schmidt rebound numbers than the typical concrete.

Table B-1: Cylinder Properties and Elastic Modulus Values

Concrete Type	Site	Age	Average Length (in.)	Average Diameter (in.)	Weight (lb)	Density (lb/ft³)	Average Freqency (Hz)	Average Elastic Modulus (ksi)
Typical	1	7 days	8.0279	3.9923	8.3585	143.7	5940.09	1958
			8.0340	3.9971	8.3375	142.9	5858.39	1897
		28 days	8.0580	4.0388	8.496	142.2	6281.34	2183
			8.0424	4.0306	8.3355	140.4	6190.05	2084
		6 months	8.0706	4.1021	8.322	134.8	6387.1	2146
			8.0988	4.0288	8.4785	141.9	6420.7	2299
		1 year	8.0278	4.0371	8.031	135.0	6036.21	1900
			8.0538	4.0400	8.244	138.0	6242.9	2090
	3	7 days	8.0151	4.0348	8.177	137.9	-	-
			8.0096	4.0284	8.316	140.8	-	-
		28 days	8.0878	4.0783	8.382	137.1	6368.54	2179
			8.0639	4.0658	8.2675	136.5	6310.84	2117
		6 months	8.0285	4.0473	8.4275	141.0	6512.79	2309
			8.0415	3.9980	8.296	142.0	6491.15	2318
		1 year	8.0288	4.0486	8.334	139.3	6498.36	2272
			8.0609	4.0359	8.415	141.0	6483.9	2308
Darkened	1	7 days	8.0259	4.0320	8.5065	143.4	5968.93	1972
			8.0158	3.9858	8.3685	144.6	5892.25	1932
		28 days	8.0284	3.9909	8.454	145.5	6218.85	2172
			8.0559	4.0414	8.514	142.4	6228.49	2147
		6 months	8.0314	3.9979	8.378	143.6	6353.41	2240
			8.0414	4.0074	8.4935	144.7	6387.1	2287
		1 year	8.0150	3.9949	8.3825	144.2	6401.5	2274
			8.0348	4.0456	8.573	143.4	6425.55	2290
	2	7 days	8.0008	4.0323	8.523	144.2	6223.69	2141
			8.0140	4.0429	8.5145	143.0	6218.88	2128
		28 days	8.0128	4.0541	8.5225	142.4	6579.29	2371
			8.0750	4.0655	8.5655	141.2	6516.8	2342
		6 months	7.9931	4.0565	8.4525	141.4	6577.7	2341
			8.0163	4.0446	8.5245	143.0	6635.4	2424
		1 year	8.0380	4.0451	8.5295	142.7	6664.25	2453
			8.0396	4.0465	8.4885	141.9	6653.19	2432

Table B-2: Loads and Compressive Strengths

Concrete Type	Site	Age	Load (lb)	Compressive Strength (psi)
Typical	1	7 days	45275	3617
			45550	3630
		28 days	64130	5006
			64950	5090
		6 months	71940	5443
			77385	6071
		1 year	77065	6020
			71825	5603
	3	7 days	49155	3845
			47920	3760
		28 days	66385	5082
			66170	5097
		6 months	74960	5827
			86310	6875
		1 year	88785	6897
			65470	5118
Darkened	1	7 days	48695	3814
			51180	4102
		28 days	70505	5636
			68405	5333
		6 months	68850	5485
			81470	6459
		1 year	77865	6212
			83710	6512
	2	7 days	61955	4852
			58510	4558
		28 days	80185	6212
			74715	5756
		6 months	78805	6098
			99110	7714
		1 year	91320	7106
			101295	7877

Table B-3: Rapid Chloride Permeability Values and Classifications

Concrete Type	Site	Age	Rapid Chloride Permeability (coulombs)	Rapid Chloride Permeability Classification
Typical	1	28 days	1906	Low
			2106	Low
		6 months	471	Very Low
			503	Very Low
		1 year	382	Very Low
			374	Very Low
	3	28 days	1175	Low
			1899	Low
		6 months	372	Very Low
			387	Very Low
		1 year	620	Very Low
			395	Very Low
Darkened	1	28 days	-	-
			-	-
		6 months	461	Very Low
			433	Very Low
		1 year	338	Very Low
			348	Very Low
	2	28 days	-	-
			-	-
		6 months	330	Very Low
			282	Very Low
		1 year	290	Very Low
			321	Very Low

Table B-4: Thermal Conductivity and Temperature

Condition	Test Location		Typical Thermal Conductivity (W/m*K)	Typical Temperature (°F)	Darkened Thermal Conductivity (W/m*K)	Darkened Temperature (°F)
Wet	Top	1	4.151	70.70	4.249	70.99
		2	3.276	70.83	3.859	70.36
		3	4.760	69.91	3.734	70.81
	Bottom	1	3.946	71.73	4.450	72.54
		2	4.647	71.82	4.351	72.01
		3	3.836	71.82	4.108	72.05
Dry	Top	1	3.068	72.34	3.216	72.50
		2	3.183	72.48	3.233	72.66
		3	3.061	72.61	3.224	72.82
	Bottom	1	3.617	72.55	4.100	72.82
		2	3.76	72.68	3.777	73.08
		3	3.255	72.79	3.832	73.18
Low-Temperature	Top	1	3.524	6.31	4.092	6.78
		2	3.725	6.15	5.019	6.04
		3	3.414	6.19	4.284	6.10
	Bottom	1	4.326	5.83	5.651	6.37
		2	4.576	5.86	4.899	5.90
		3	4.871	5.94	6.718	5.86
High-Temperature	Top	1	1.364	152.26	2.604	155.35
		2	1.786	154.35	1.876	155.08
		3	2.626	152.89	2.286	154.69
	Bottom	1	3.004	148.30	1.350	151.83
		2	3.449	150.69	2.902	99.03
		3	3.384	151.95	3.313	153.45

Table B-5: Average Schmidt Rebound Hammer Values

Concrete Type	Test Location	Condition			
		Wet	Dry	Low-Temperature	High-Temperature
Typical	Top	26.0	32.0	37.5	36.0
		30.5	30.0	37.5	36.0
		30.0	36.0	38.5	38.5
	Bottom	33.0	31.5	36.5	38.5
		38.0	32.0	35.5	33.5
		32.5	48.0	34.0	38.5
Darkened	Top	40.5	45.5	44.0	44.0
		41.0	46.0	40.0	36.0
		42.5	36.5	41.5	38.0
	Bottom	40.0	38.0	42.5	39.8
		33.0	32.5	43.5	42.0
		34.5	34.0	42.0	39.5